UNIVERSIDAD DE CHILE
FACULTAD DE CIENCIAS FÍSICAS Y MATEMÁTICAS
DEPARTAMENTO DE INGENIERIA DE MINAS

MODELAMIENTO DE INCERTIDUMBRE EN EL DISEÑO DE UNIDADES GEOLÓGICAS MEDIANTE SIMULACIÓN IMPLÍCITA DE CONTACTOS CONSIDERANDO UN MODELO GEOLÓGICO INTERPRETATIVO PREEXISTENTE

TESIS PARA OPTAR AL GRADO DE MAGISTER EN MINERÍA

RENATO ANDRES FERRER AYALA

PROFESOR GUÍA:
XAVIER EMERY

MIEMBROS DE COMISIÓN:
NADIA MERY GUERRERO
FELIPE NAVARRO VARGAS
MOHAMMADALI MALEKITEHRANI

SANTIAGO DE CHILE
2022

RESUMEN DE LA TESIS PARA OPTAR
AL GRADO DE: Magíster en Minería
POR: Renato Andres Ferrer Ayala
FECHA: Enero 2022
PROFESOR GUÍA: Xavier Emery

MODELAMIENTO DE INCERTIDUMBRE EN EL DISEÑO DE UNIDADES GEOLÓGICAS MEDIANTE SIMULACIÓN IMPLÍCITA DE CONTACTOS CONSIDERANDO UN MODELO GEOLÓGICO INTERPRETATIVO PREEXISTENTE

Se propone un algoritmo de simulación implícito que utiliza funciones de distancia definidas para representar la configuración geológica en el subsuelo mientras se tienen en cuenta dos fuentes de información: los datos del pozo de perforación considerados como información 'dura' (libre de errores) y un modelo geológico interpretativo preexistente visto como información 'suave'. El algoritmo propuesto sigue un flujo de trabajo jerárquico y se basa en el cálculo de la distancia a lo largo del sondaje entre los datos de cada pozo de perforación y el límite geológico más cercano (variable primaria), junto con la distancia omnidireccional entre cada nodo del modelo interpretativo y el límite más cercano (covariable). El nivel de influencia de estos últimos sobre los primeros se puede controlar ajustando su correlación cruzada, de modo que se pueda aumentar o reducir el efecto de la interpretación geológica en la simulación, dependiendo de la confianza del experto en dicha interpretación. Los parámetros clave para una implementación exitosa del enfoque propuesto son la elección de un árbol binario para controlar las relaciones topológicas entre las unidades geológicas simuladas, de un modelo de correlación espacial para controlar la continuidad geológica y la regularidad de los límites, y de un coeficiente para controlar la confiabilidad dada a los datos blandos. La especificación de estos parámetros puede evaluarse mediante consideraciones geológicas y mediante técnicas de validación cruzada. La propuesta se aplica a un caso de estudio sintético y un caso real que corresponde al pórfido cuprífero de Spence, donde se demuestra que la incorporación de datos blandos permite reproducir zonificaciones geológicas en áreas con pocos datos de perforación. También se discuten algunos problemas de implementación y posibles mejoras del método.

SUMMARY OF THE THESIS TO OPT FOR THE DEGREE OF: Master in Mining
BY: Renato Andres Ferrer Ayala
DATE: January 2022
GUIDE PROFESSOR: Xavier Emery

MODELING THE UNCERTAINTY IN THE LAYOUT OF GEOLOGICAL UNITS BY IMPLICIT BOUNDARY SIMULATION ACCOUNTING FOR A PREEXISTING INTERPRETIVE GEOLOGICAL MODEL

An implicit simulation algorithm that uses signed distance functions is proposed to represent the geological configuration in the subsurface while accounting for two sources of information: drill hole data considered as 'hard' (error-free) information, and a preexisting interpretive geological model viewed as 'soft' information. The proposed algorithm follows a hierarchical workflow and relies on the calculation of the down-the-hole distance between each drill hole data and the closest geological boundary (primary variable) together with the omnidirectional distance between each node of the interpretive model and the closest boundary (covariate). The level of influence of the latter on the former can be controlled by tuning their cross-correlation, so that one can increase or reduce the effect of the geological interpretation in the simulation, depending on the confidence of the expert in such an interpretation. The key parameters for a successful implementation of the proposed approach are the choice of a binary tree to control the topological relationships between the simulated geological units, of a spatial correlation model to control the geological continuity and the boundaries regularity, and of a coefficient to control the trustworthiness given to the soft data. The specification of these parameters can be assessed by geological considerations and by cross-validation techniques. The proposal is applied to a synthetic and a real case study, where it is shown that the incorporation of soft data allows reproducing geological zonations in areas with few drill hole data. Some implementation issues and possible improvements to the method are also discussed.

TABLA DE CONTENIDO

CAPÍTULO PRIMERO

1. INTRODUCCIÓN

1.1. PREÁMBULO

En proyectos mineros, la estimación de recursos minerales tanto en tonelaje como en ley de commodities es de vital importancia. Los métodos utilizados para la estimación son en la mayoría de los casos interpoladores lineales, siendo el "Kriging" uno de los más conocidos y utilizados. Este interpolador entrega una solución única en la estimación, lo que normalmente se suele llamar un método determinístico. Sin embargo, otro de los análisis requeridos en minería es la cuantificación de incertidumbre de dichos recursos minerales, pero los métodos determinísticos no son los más adecuados para este propósito. Es así como la utilización de métodos estocásticos para la estimación y cuantificación de incertidumbre en minería cada vez toma más relevancia y su entendimiento es crucial en los equipos de trabajo del área de geología.

La cuantificación de la incertidumbre geológica en variables regionalizadas se realiza hoy en día con simulaciones geoestadísticas. El por qué son utilizadas, se debe a que ningún modelo de interpolación logrará reproducir la realidad sin error. En general, en procesos naturales nunca existirá un muestreo exhaustivo tal como ocurre en procesos geológicos y aunque son entendidos en términos genéticos, son muy complejos de predecir en el espacio. Las simulaciones pueden construir una distribución de posibles escenarios, todos y cada uno de ellos tan posible como el otro, lo que permite conocer las probabilidades de ocurrencia de ciertos eventos.

1.2. MOTIVACIÓN

Existen diversas metodologías para la construcción de simulaciones geoestadísticas, sin embargo, la simulación de variables categóricas relacionadas a atributos geológicos es algo más complejo. En términos geológicos, los contactos de las unidades geológicas podrían tomar formas que son muy difíciles de predecir solo a partir de métodos numéricos y mucho más complejo lejos de los datos. En este campo han existido distintos enfoques, todos ellos muy prácticos de utilizar, pero con algunas desventajas a la hora de reproducir una incertidumbre "plausible" de los bordes de contactos en zonas alejadas de los datos. Es por ello, que la motivación principal en este trabajo

de tesis es la exploración de métodos numéricos que permitan acercar más la geología con los procesos estocásticos.

1.3. OBJETIVOS DEL ESTUDIO

El objetivo principal es diseñar un método de simulación de contactos geológicos que tenga en cuenta dos fuentes de información: datos de muestreo como variable primaria (duros) y datos de una interpretación geológica 3D preexistente como covariable (blandos). De particular interés será la elaboración de un modelo donde la covariable pueda correlacionarse espacialmente con la variable primaria y, al mismo tiempo, donde los modeladores puedan controlar el nivel de confianza de los datos blandos.

Lograr este objetivo requiere de la realización de múltiples etapas, las que en términos conceptuales ya han sido abordadas en trabajos previos. Sin embargo, en esta tesis se plantea un nuevo enfoque metodológico que logrará dar solución a algunos de los problemas que se presentan con métodos tradicionales.

Metodologías como ésta permiten analizar y cuantificar la incertidumbre asociada a atributos geológicos que controlan las variables de interés económico en un proyecto minero, y que afectan principalmente al tonelaje de recursos minerales.

1.3.1. Objetivos Específicos

Para diseñar un método de simulación, se debe tener en cuenta aspectos sobre la naturaleza de la variable, el tipo de variable, la forma en cómo se utiliza, la base teórica y los parámetros que definirán su resultado.

En general, los métodos existentes han trabajado en dos líneas metodológicas, ambas con transformaciones de datos categóricos en numéricos, pero uno es de indicadores y el otro de distancias. De este último, el cual ha sido utilizado ampliamente por la industria, se ha notado levemente una falencia en velocidad y robustez. Debido a lo anterior, también se incluirá la implementación de nuevos criterios en el cálculo de distancias que eviten algunas inconsistencias de los métodos tradicionales.

Otro de los problemas en métodos tradicionales es la consideración de información blanda en sus algoritmos de simulación. Actualmente todos se basan simulaciones directas, sin embargo, una forma de abordar mucho mejor el problema es realizando una co-simulación y no solo eso, sino que controlar el grado de correlación que existe entre ambas fuentes de información entregará una herramienta muy práctica y consistente a aquellos modeladores que buscan reflejar la incertidumbre en sus simulaciones.

Dado lo anterior, se propone:

- Trabajar con dos casos de estudio: uno sintético creado para probar la metodología y uno real correspondiente al depósito de Spence.
- Para ambos casos los datos iniciales serán categóricos, que representan mediante una codificación definida, los distintos atributos geológicos presentes.
- Los datos serán transformados a una variable numérica a través de una función de distancia entre unidades geológicas.
- El método de simulación a utilizar se basa en el modelo multigaussiano con un algoritmo de bandas rotantes.
- Se creará un parámetro que define la correlación entre la variable primaria (datos de muestreo) y secundaria (modelo interpretativo preexistente).
- Implementar un método de validación cruzada.

1.4. ALCANCES DE LA INVESTIGACIÓN

Aspectos relacionados tanto a la construcción de la nueva metodología como a su implementación en un caso sintético y uno real son parte del alcance de esta tesis de magister, incluidos:

- La programación de los algoritmos y el entendimiento de los cálculos matemáticos necesarios para alcanzar los objetivos.
- Evaluación y validación del método, con caso sintético y real.

1.5. METODOLOGÍA GENERAL DEL ESTUDIO

1.5.1. Modelamiento Implícito de Contactos

Consideremos solo dos unidades geológicas (A y B) mapeadas en una base de datos de sondajes compositada. En cada punto de la unidad A, se calcula la distancia al punto más cercano en la unidad B. Lo mismo se hace para la unidad B, asignando un signo negativo a las distancias calculadas. Ahora, se tiene una base de datos con coordenadas espaciales y una propiedad numérica (distancia). El traspaso de estas variables categóricas a numéricas utilizando la función de distancia es útil para simular el límite de unidades geológicas en el espacio (McLennan & Deutsch, 2006; Carr et al., 2001)

El límite entre las dos unidades suele ser más irregular, en la medida en que las técnicas de simulación no suavizan la realidad como lo hace la interpolación como el Kriging. Además, este enfoque es estocástico y proporciona múltiples soluciones igualmente probables, llamadas "resultados" o "realizaciones".

1.5.2. Modelamiento Jerárquico

En caso de existir más de 2 unidades geológicas, se debe primero definir una estrategia de simulaciones binarias a través de un árbol de clasificación. Esto se debe a que los métodos de simulación solo son capaces de simular un límite a la vez, por lo tanto, es importante definir una jerarquía de orden y espacio para simular cada una de ellas. Las consideraciones de este árbol binario suelen ser las siguientes: 1) edad de las unidades geológicas, 2) volumen de las unidades geológicas, 3) importancia de las unidades geológicas y 4) relaciones de corte entre unidades (Madani y Emery, 2015).

1.5.3. Cálculo de la función de distancia entre unidades geológicas

Como se indicó anteriormente, la simulación de límites geológicos se basa en la simulación de la distancia entre dos unidades geológicas. Para ello, esta tesis propone el cálculo simultáneo de dos funciones de distancia, donde la primera corresponde al cálculo en los datos de sondajes

(información dura) y la segunda al cálculo en los datos del modelo interpretativo preexistente (información blanda).

En el primer caso, se considera la distancia solo entre datos de sondaje para dos unidades geológicas distintas y metodológicamente se realiza a lo largo del sondaje (comúnmente llamado "down-the-hole"). Si utilizáramos por el contrario una función de distancia omnidireccional, se produce uno de los primeros problemas de los métodos tradicionales, y es que cada vez que un sondaje se añada a la base de datos la función de distancia cambiará en todo el dominio (lo que no es un efecto deseado). En el segundo caso, se considerará la distancia tanto entre sondajes como entre el modelo interpretativo con una metodología omnidireccional. Dado que el modelo es una grilla regular en todo el dominio, no hay problema en aplicar este método ya que la única forma que cambie la función es que el modelo sea actualizado (lo que es sensato).

1.5.4. Transformación de distancias

Las dos distancias calculadas se deben transformar a valores normales con el objetivo de poder utilizar los métodos de simulación multigaussiana. Este método es estándar en los procesos de simulación geoestadística.

1.5.5. Modelamiento de las variables de distancia

La estructura de correlación espacial conjunta de ambas distancias (de sondajes y del modelo interpretativo) se puede inferir calculando sus covarianzas o variogramas directos y cruzados, y luego ajustando un modelo de corregionalización. Dado que ambas distancias son calculadas basadas en la misma información original, se espera que su correlación sea alta. De este modo, si la correlación es máxima, el grado de influencia del modelo interpretativo será alto y por tanto la incertidumbre asociada a la simulación será baja en todo el dominio. De lo contrario si la correlación es nula, entonces lejos de los datos la incertidumbre será muy alta ya que no hay ningún control más que los datos de sondaje.

La propuesta de esta tesis es incluir un parámetro que pueda controlar el grado de correlación que existe entre ambas distancias y, de este modo, el modelador tendrá un el control sobre el nivel de influencia que tendrá el modelo interpretativo sobre la simulación. Este parámetro

variará en la escala 0 a 1, donde 0 indica que la correlación es nula y 1 indica que la correlación es máxima. La elección del valor de este parámetro puede estar basado en el conocimiento geológico del modelador o puede ser ajustado por validación cruzada.

1.5.6. Simulación conjunta

La simulación conjunta de estas dos variables será realizada con un algoritmo espectral (Emery et al., 2016), condicionado a los datos de los sondajes y al modelo interpretativo. Luego, la simulación será devuelta a su escala original donde se podrá realizar una truncación a la distancia 0 que definirá el límite de dos unidades geológicas para cada una de las realizaciones.

1.6. ESTADO DEL ARTE

1.6.1. Geoestadística y estimación de recursos

La geoestadística puede ser definida como la aplicación de modelos probabilísticos a variables regionalizadas (Chilès & Delfiner, 2012). En la práctica, puede ser aplicada a cualquier variable continua que presente una estructura en el espacio. Por su parte, Pyrcz & Deutsch (2014) definen a la geoestadística como una rama de la estadística aplicada que difiere de la estadística en tres aspectos básicos:

1. Se centra en el estudio de variables geolocalizadas (usualmente ligada a la geología por los procesos naturales que involucran).
2. Modelamiento y tratamiento explícito de la correlación espacial entre los datos.
3. Tratamiento de los datos a diferentes volúmenes y niveles de precisión.

Típicamente el objetivo es estudiar una variable regionalizada para determinar su comportamiento en el espacio y poder estimar su valor en sitios donde no se posee información acerca de ella. En minería, el estimador utilizado por excelencia es el kriging, el cual es un estimador lineal insesgado que minimiza la varianza del error. Con los datos de sondajes in-situ, se realiza un análisis estadístico y geológico del depósito con el fin de definir las unidades de estimación. En estas unidades se realiza un análisis variográfico independiente para obtener el variograma de los datos, el cual es considerado una medida confiable de la correlación espacial de los datos. Finalmente, se realiza la etapa de kriging para obtener una estimación de los recursos del yacimiento en estudio (Journel & Huijbregts, 1978).

A pesar de que, por construcción, kriging es el mejor estimador lineal insesgado, la varianza de kriging no refleja de forma adecuada la incertidumbre asociada a la estimación. El principal defecto de este estimador es que la varianza del error no depende de los valores de los datos: depende solo de su configuración geométrica y de la estructura espacial de la variable regionalizada en estudio. Es así como sectores donde los datos toman valores cercanos entre ellos pueden no presentar una varianza diferente comparada con zonas donde los datos son más erráticos, siempre y cuando presenten la misma configuración geométrica. De esta forma, este estadístico no refleja el llamado efecto proporcional, el cual se ve cuando las zonas de valores altos de la variable muestran más variabilidad que las zonas de valores bajos.

La estimación de kriging representa un modelo determinístico asociado al mejor valor esperado en cada uno de los nodos estimados. Sin embargo, la cuantificación de la incertidumbre y riesgo es analizada a partir de las simulaciones geoestadísticas, que representan un modelo estocástico, asociado a la distribución de probabilidad de la variable en cada uno de los nodos simulados.

1.6.2. Simulación geoestadística

La simulación, a diferencia de kriging no es precisa, es decir, no minimiza el error pues se centra en respetar las estadísticas de la variable regionalizada (Chilès & Delfiner, 2012). Esto permite que en una simulación los valores no se vean suavizados como en el kriging. Estas propiedades de la simulación permiten utilizar las diferentes realizaciones para hacer un análisis de riesgo sobre los modelos obtenidos, estudiar la sensibilidad de la variable y colocarse en distintos escenarios. Este tipo de simulación se utiliza tanto para variables continuas como para discretas cuantificables o categóricas, que es el principal enfoque de esta tesis. Si bien es cierto las variables categóricas no son atributos continuos, existen transformaciones a fin para poder llevar las categorías a una distribución continua cuya correlación espacial será definida por el variograma de los datos transformados.

Las simulaciones son básicamente métodos matemáticos que describen un fenómeno natural intentando traspasar todas las propiedades de la muestra a la población como la distribución, variabilidad y correlación espacial.

$$\forall z \in \mathbb{R}, F(z) = Prob[Z(x) < z] \qquad (1)$$

Como primer enfoque de incertidumbre, se puede considerar la distribución global (ecuación 1). Sea Z la función aleatoria que representa una variable regionalizada de interés, y x un punto del espacio no muestreado, la función de distribución F(z) se define como la probabilidad de que la variable aleatoria Z(x) sea menor a un umbral de corte. Bajo el supuesto de estacionaridad, esta distribución es invariante en el espacio, es decir no depende del punto x.

$$\forall z \in \mathbb{R}, F(x; z|datos) = Prob[Z(x) < z|Z(x_1), \dots Z(x_n)] \qquad (2)$$

El segundo enfoque es el de incertidumbre local, el que añade a la definición anterior el concepto de condicionamiento a los datos cercanos (ecuación 2). En particular, si la distancia entre el nodo simulado y una muestra de la variable es 0, entonces la simulación entregará como resultado el mismo valor de la muestra y no existirá incertidumbre. Este tipo de simulaciones son llamadas condicionales y son las principales usadas en el campo de cuantificación de incertidumbre en minería.

La simulación como algoritmo, generalmente se aplica a variables numéricas continuas. La aplicación a variables categóricas requiere de una transformación adicional hacia valores numéricos. En el estado del arte actual estas transformaciones son hacia indicadores o distancias al contacto. Luego, son nuevamente transformadas pero esta vez a una distribución gaussiana con media 0 y varianza 1. La simulación en sí misma, es realizada por algoritmos ya validados y conocidos en la industria y la academia, como lo son el método secuencial gaussiano y el de bandas rotantes. Finalmente, se necesita un último paso de transformación de vuelta al espacio real de los datos, para luego ser interpretadas como variables categóricas y no continuas.

1.6.3. Simulación de variables categóricas

Desde el punto de vista de metodologías de simulación, al presente se pueden encontrar:

- Simulación Secuencial de Indicadores: Consiste en codificar los datos según una función indicador. Con esta información se genera el variograma del indicador, luego se define un camino aleatorio con los lugares no muestreados visitándolos sólo una vez. Se modela la distribución condicional en una posición no muestreada usando kriging de indicadores y se

obtiene el valor simulado al sortear un valor según dicha distribución condicional. Se debe codificar el nuevo valor obtenido para usarlo en la determinación de las siguientes posiciones (Remy, et al. 2009).

- Simulación Gaussiana Truncada: Con este método las variables categóricas, como las unidades geológicas, no son simuladas directamente, sino que se simula una función aleatoria gaussiana primero y luego ésta se transforma en la variable unidad geológica, por truncación (Matheron, et al. 1987).

- Simulación Plurigaussiana: Corresponde a la generalización del método anterior de gaussianas truncadas. En este caso, las categorías deben estar ordenadas según sus relaciones de contacto, lo que es definido a través de una regla o de la bandera de truncación. Esto otorga más flexibilidad a la hora de simular varias unidades geológicas, sin embargo, ciertas configuraciones geológicas complejas son difíciles de reproducir (Galli, et al. 1994).

- Simulación Multipunto: Para aplicar esta metodología se debe definir un patrón, que corresponde a un conjunto de pixeles o puntos (nodos), cada uno con valor(es) de una o más variables, ordenados espacialmente de tal forma que se puedan diferenciar de otros patrones con ordenamiento distinto. Una imagen de entrenamiento representa el fenómeno geológico que genera la estructura espacial de la variable y a partir de ella se realiza la inferencia (Strebelle, 2002).

- Simulación de Distancias al Contacto: McLennan & Deutsch (2006) acuñaron el término *BOUNDSIM*, como un método de simulación de variables categóricas que consiste en simular las distancias a los contactos entre unidades. Esta función de distancias ya había sido estudiada con anterioridad y Carr et al. (2001) lo publica utilizando el método con funciones de radio basal (RBF) lo que llevó a la generación de uno de los softwares de modelamiento geológico más utilizados en la industria minera, Leapfrog.

De los métodos descritos, dos de ellos son los más utilizados en el análisis de incertidumbre geológica en minería: la simulación plurigaussiana y la simulación de distancias al contacto. Cualquiera sea el método, ante mucha información de sondajes no tendrá grandes problemas en la

generación de escenarios plausibles. Sin embargo, cuando existen zonas sin mucha información es cuando se producen inconsistencias o escenarios poco fidedignos. Dentro de ellos los más relevantes son los cambios por nueva información y las inconsistencias geológicas ante poca información. Deutsch (2006) utilizó el modelo geológico determinístico como base para que estos problemas fueran más suavizados, acuñando el término LVM (Local Varying Mean).

Luego de la entrada de este método, en general se ha tendido a usar como una referencia en la industria considerando a la simulación de distancias al contacto con el uso de LVM como uno de los más importantes, aunque aún con cierto grado de falencias que no han sido consideradas.

1.7. RESUMEN DE LA INVESTIGACIÓN

Los resultados de este estudio serán presentados a través del siguiente artículo científico, publicado en 2021 en la revista Natural Resources Research:

Art.1: Ferrer, R., Emery, X., Maleki, M. et al. Modeling the Uncertainty in the Layout of Geological Units by Implicit Boundary Simulation Accounting for a Preexisting Interpretive Geological Model. Natural Resources Research (2021). https://doi.org/10.1007/s11053-021-09964-9.

CAPÍTULO SEGUNDO

2. RESULTADOS

2.1. ARTÍCULO 1

Natural Resources Research (© 2021)
https://doi.org/10.1007/s11053-021-09964-9

Original Paper

Modeling the Uncertainty in the Layout of Geological Units by Implicit Boundary Simulation Accounting for a Preexisting Interpretive Geological Model

Renato Ferrer,[1,2,3] Xavier Emery,[2,3] Mohammad Maleki,[4,5] and Felipe Navarro[2]

Received 4 May 2021; accepted 29 September 2021

An implicit simulation algorithm that uses signed distance functions is proposed to represent subsurface geological configuration while accounting for two sources of information: drillhole data considered as 'hard' (error-free) information and a preexisting interpretive geological model viewed as 'soft' information. The proposed algorithm follows a hierarchical workflow and relies on the calculation of the down-the-hole distance between every drillhole data and the closest geological boundary (primary variable) together with the omnidirectional distance between each node of the interpretive model and the closest boundary (covariate). The level of influence of the latter on the former can be controlled by tuning their cross-correlation so that one can increase or reduce the effect of the geological interpretation in the simulation, depending on the confidence of the expert in such an interpretation. The key parameters for a successful implementation of the proposed approach are the choice of a binary tree to control the topological relationships between the simulated geological units, of a spatial correlation model to control the geological continuity and the boundaries regularity, and of a coefficient to control the trustworthiness given to the soft data. The specification of these parameters can be assessed by geological considerations and by cross-validation techniques. The proposal was applied to a synthetic and a real case study, where it was shown that incorporation of soft data allowed reproduction of geological zonations in areas with few drillhole data. Some implementation issues and possible improvements to the method are also discussed.

KEY WORDS: Geomodeling, Geological uncertainty, Geological interpretation, Implicit modeling, Signed distance functions.

INTRODUCTION

In geosciences and natural resources engineering, subsurface geological units such as lithology, hydrothermal alteration and ore mineralized domains are modeled usually prior to the prediction or simulation of quantitative regionalized variables (e.g., metal grades, mineral percentages, rock porosity and permeability) based on the fact that the former have a spatial control on the latter (Journel & Huijbregts, 1978; Dubrule, 1993; Armstrong et al.,

[1]BHP Billiton, Santiago, Chile.
[2]Advanced Mining Technology Center, University of Chile, Santiago, Chile.
[3]Department of Mining Engineering, University of Chile, Santiago, Chile.
[4]Departamento de Ingeniería Metalúrgica y Minas, Universidad Católica del Norte, Antofagasta, Chile.
[5]To whom correspondence should be addressed; e-mail: mohammad.maleki@ucn.cl

Published online: 22 October 2021

2011; Chilès & Delfiner, 2012; Emery and Maleki, 2020; Emery & Séguret, 2020). Many approaches are currently available for delineating geological units based on expert knowledge and sampling information (e.g., drillhole data, surface maps, geophysical information). Among these approaches, one can distinguish between deterministic approaches, which provide a single subsurface interpretation (Aug et al., 2005; Calcagno et al., 2008; Cowan et al., 2003; Mallet, 2002; Royer et al., 2015; Wellmann & Caumon, 2018, among others), and stochastic simulation approaches, which generate multiple outcomes from which one can assess the uncertainty in geological boundaries and its impact on resources modeling, production planning, prefeasibility and feasibility studies (Berry & McCarthy, 2006; Li et al., 2008; Maleki et al., 2020; McCarthy, 2003). The latter approaches include indicator (Alabert, 1987), transition probability-based (Carle & Fogg, 1997), object-based (Benito Garcia-Morales et al., 2003; Lantuéjoul, 2002), process-based (Rivoirard et al., 2008), truncated Gaussian (Matheron et al., 1987), plurigaussian (Armstrong et al., 2011), multiple-point (Mariethoz & Caers, 2014) and implicit boundary (Amarante et al., 2021; Cáceres et al., 2011; Deutsch & McLennan, 2007; Henrion et al., 2010) simulation.

Implicit boundary simulation, which is the main concern of this work, combines traditional implicit boundary modeling, which was introduced in the computer graphic field (Carr et al., 2001; Turk and O'Brien, 2002), with geostatistical simulation in order to generate outcomes of geological units and to define the uncertainty in the layout of each geological unit (see section **Implicit Boundary Modeling** below). In this approach, the following steps were used to generate outcomes of two complementary geological units (indexed by A and B):

- Step 1. For every sampling data, the signed distance to the nearest sample data belonging to the other unit was calculated. This distance is positive if the sampling data belong to unit A and is negative if it belongs to unit B.
- Step 2. The signed distances were transformed into Gaussian equivalents (normal scores).
- Step 3. Variogram analysis was performed on the normal scores data.
- Step 4. The transformed distance was simulated in the study area, conditioned to the normal scores data, and back-transformed to the original signed distance.
- Step 5. The two units were obtained by considering the set of locations where the simulated distance was positive or negative, respectively.

The previous workflow is parenthetical to that of truncated Gaussian or plurigaussian simulation (Armstrong et al., 2011), where the units are obtained by truncating latent Gaussian random fields, the difference being that, here, these random fields are associated with the signed distances to the unit boundaries and are 'observable.'

In densely sampled areas, there is usually no problem to accurately delineate boundaries of geological units. However, when moving away from these areas, the level of confidence decreases and it is often the geologist who proposes an interpretation of the unit boundaries, based on his/her expert knowledge. To be realistic and to reproduce stratigraphic relationships, geological trends, zonations, or faults, geostatistical simulation methods should therefore be able to carefully account for the geological interpretation ('soft' information) and not just the sampling information ('hard' data). To this end, one strategy is to introduce expert knowledge via topological, chronological or geological rules (Calcagno et al., 2008; de la Varga et al., 2019; Madani & Emery, 2015), or by adapting the parameters of the stochastic model, e.g., using spatially varying mean values for unit indicators in sequential (Alabert, 1987; Deutsch, 2006), multiple-point (Høyer et al., 2017; Mariethoz & Caers, 2014), plurigaussian (Beucher et al., 1993; Madani & Emery, 2015; Ravenne et al., 2002) or object-based (Beucher et al., 2005) simulation. This strategy has been proposed for implicit boundary simulation, too, by introducing a spatially varying mean value for the signed distance function (Henrion et al., 2010).

An alternative approach to account for expert geological knowledge is to complement hard sampling data by secondary data that constrain the layout of geological units, e.g., orientation data or geophysical data. The incorporation of such secondary data, which originate from remote sensing or field observations, has already been proposed in implicit boundary modeling (Calcagno et al., 2008; Caumon et al., 2013; Chilès et al., 2004; de la Varga et al., 2019; Gonçalves et al., 2017; Hillier et al., 2014; Jessell et al., 2010; Lajaunie et al., 1997; Manchuk & Deutsch, 2019; Maxelon et al., 2009;

Vollgger et al., 2015; Wellmann et al., 2014), and in plurigaussian (Emery, 2007) and transition probability-based (Carle & Fogg, 2020; Koch et al., 2014) simulation. In all these approaches, one of the main difficulties is to quantify how reliable secondary data are, as in general they cannot be treated as being 100% accurate or certain, while hard data are often considered as error-free.

The objective of this paper is to design an implicit boundary simulation method that accounts for two sources of information: 'hard' sampling data, which provide the primary variable to be simulated (a categorical variable codifying geological units), and 'soft' data from an interpretive geological model to be included as a covariate. Of particular interest is the elaboration of a model where the covariate can be spatially cross-correlated with the primary variable and, at the same time, where modelers can control the level of confidence of the soft data. Our proposal is detailed in the following section, and it is applied to a synthetic and a real case study. Both case studies have been developed with computer scripts written in Python and GNU Octave languages. A general discussion is given and conclusions follow.

PROPOSED METHODOLOGY

Implicit Boundary Modeling

To understand the method, let us consider just two geological units (A and B) mapped in a drillhole database. First, the data should ideally be composited into down-the-hole intervals of the same length. Then, at each point in unit A, the distance to the nearest point in unit B is calculated. The same is done for unit B. The distances for the data of unit A are indicated with a positive sign, and a negative sign for that of unit B. Now, one has a database with spatial coordinates and a numerical property (signed distance). This information can be used finally to model the unit boundary on a defined volume composed of a regular grid, by means of spatial interpolation techniques such as kriging or radial basis functions, but it can also be used to simulate the unit boundary on the same volume.

In the interpolation case, the result corresponds to a prediction of the signed distance at each grid node, where positive values will be classified as part of unit A and negative values as part of unit B. Because interpolators do not reproduce the spatial variability of the input data, the result is usually a representation of what is most likely to be expected. This approach is deterministic and provides only one solution. When carried out in a real geological modeling scenario, this process defines an interpretive geological model.

In the simulation case, the boundary between the two units is usually more irregular, because simulation techniques do not smooth out the reality as interpolation does. This approach is stochastic and provides multiple equally probable solutions, called 'outcomes' or 'realizations.'

Hierarchical Modeling

In the presence of more than two geological units, implicit boundary simulation often works in a hierarchical way: one unit is simulated first, then a second unit is simulated in the complement of the first one, and so on. Accordingly, the first step is to define the order (through a binary tree) in which geological units will be simulated, which can be done based on geological considerations of the genesis and age of the units (Madani & Emery, 2015): A younger unit can crosscut an older one; therefore, it should be placed upstream in the binary tree, while the reverse is not allowed (Fig. 1).

The implicit boundary simulation problem, therefore, reduces to a set of binary simulations (one unit with respect to its complement). To obtain realizations that agree with the knowledge of the subsurface, it is of interest to incorporate two sources of conditioning data. On the one hand, 'hard' data originating from geological core logging, where the prevailing unit has been continuously observed along drillholes; on the other hand, 'soft' data from an interpretive geological model based on expert knowledge. Next, a joint simulation approach is proposed to account for both types of data.

Shortest Down-the-Hole and Omnidirectional Distances to Unit Boundary

Implicit boundary modeling relies on the calculation of a signed distance between each sample or target location and the closest unit boundary. In our proposal, two such distances (denoted as Z_1 and Z_2) are defined, one for the hard data and the other for the soft data. The first one (Z_1) considers, for every

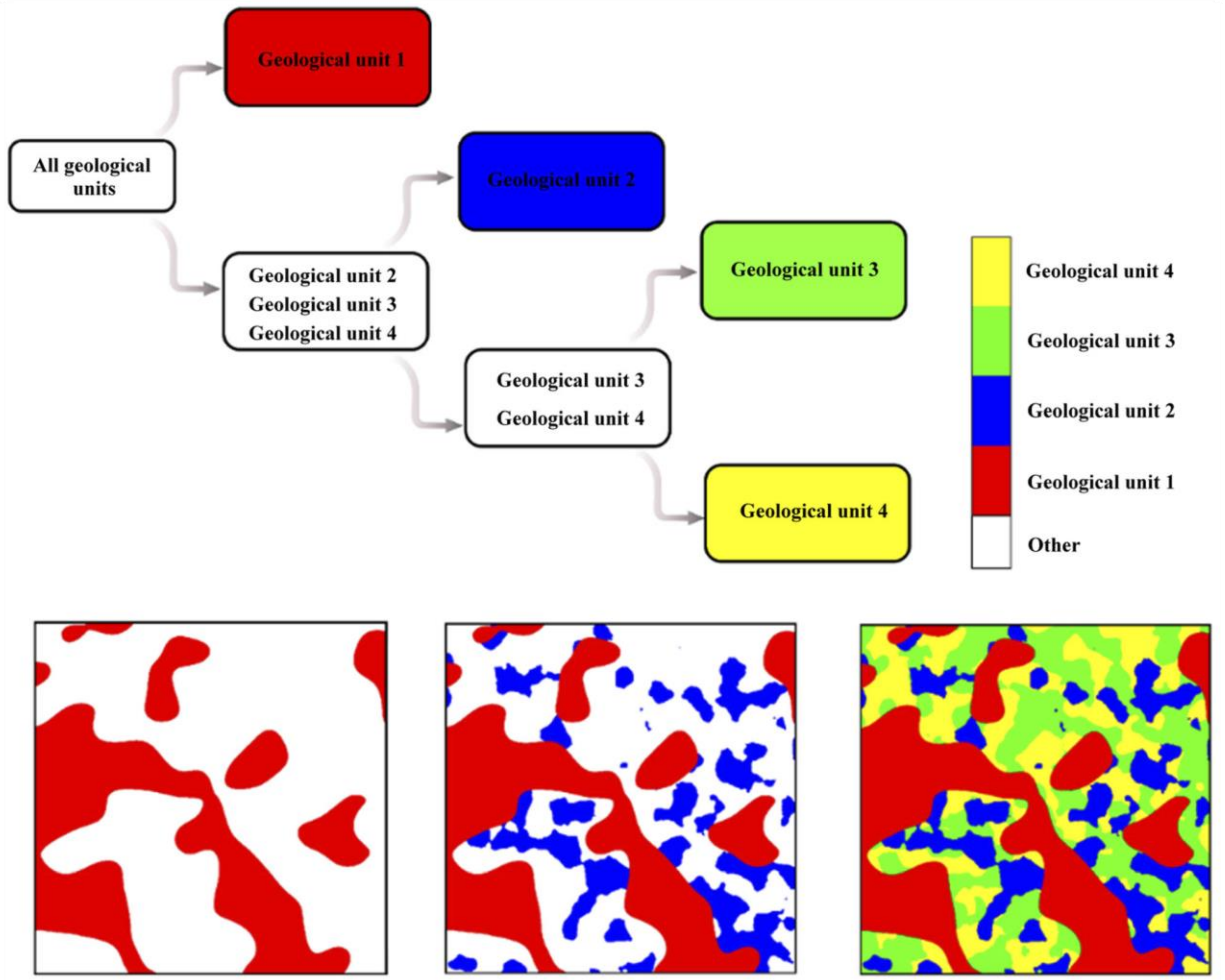

Figure 1. Example of binary tree (top) and hierarchical simulation (bottom) of four geological units. Modified from Maleki et al., (2016).

drillhole data, the distance to the closest data of the same drillhole that belongs to the complementary unit (Fig. 2a). It should be pointed out that this distance Z_1 is calculated along the drillhole and not another direction in order to avoid any ambiguity in the definition of the variable: in particular, Z_1 will not change even after adding more drillholes. In contrast, the second distance (Z_2), calculated both for the drillhole data and the nodes of the interpretive geological model, is defined as the omnidirectional distance to the closest node that belongs to the complementary unit in the interpretive model (Fig. 2b). Because this model is known exhaustively, here again there is no ambiguity in the definition of this omnidirectional distance.

Normal Scores Transformation

The two calculated distances (Z_1 and Z_2) are normal-score transformed in order to allow the use of Gaussian simulation algorithms (Chilès & Delfiner, 2012):

$$\begin{aligned} Z_1 &= \varphi_1(Y_1) \\ Z_2 &= \varphi_2(Y_2) \end{aligned} \tag{1}$$

where Y_1 and Y_2 are the respective Gaussian equivalents, and φ_1 and φ_2 are the associated normal scores transformation functions. Some difficulties may arise for the down-the-hole distance Z_1 when drillholes are not evenly distributed within the region under study, in which case the experimental

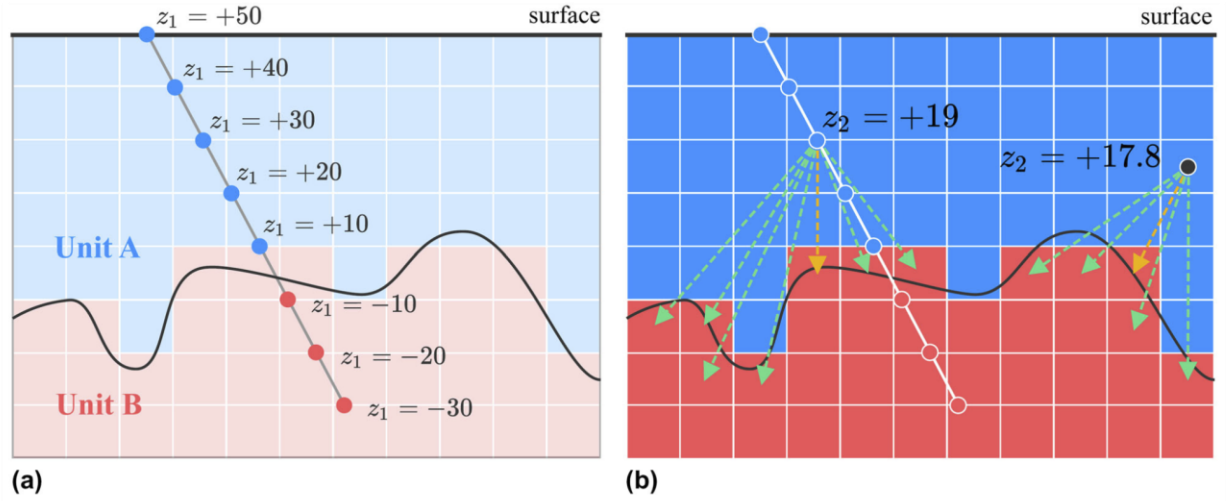

Figure 2. (**a**) Calculation of the shortest down-the-hole distance to the complementary unit for drillhole data. The gray straight line represents a drillhole, the black curve represents the boundary between units A and B, the squares represent the grid cells of the interpretive model, and the blue and red dots are the gravity centers of the drillhole data belonging to units A and B, respectively. (**b**) Calculation of the shortest omnidirectional distance to the complementary unit for a drillhole data (blue dot) and for a node of the interpretive geological model (black dot). The dotted green arrows represent the distances that can be calculated for a data or grid node, the minimum distance being represented by an orange arrow.

distribution of Z_1 may lack representativeness and the normal scores transformation function φ_1 is poorly known. To circumvent this inconvenience, one can use the interpretive model to calculate, for each node, the distance along the vertical to the closest node belonging to the complementary unit and to identify the normal scores transformation function of this vertical distance with that (φ_1) of the down-the-hole distance, assuming that most of the drillholes are vertical or sub-vertical.

Geostatistical Modeling of Y_1 and Y_2

The joint spatial correlation structure of Y_1 and Y_2 can be inferred by calculating their experimental direct and cross-covariances or variograms and fitting a coregionalization model. For instance, the latter can be obtained by a sum of basic covariances or variograms, each weighted by a positive semidefinite sill matrix (linear coregionalization model) (Chilès & Delfiner, 2012; Wackernagel, 2003). In case of having an accurate interpretive geological model, i.e., a model with no inconsistency with the drillhole data, and vertical or sub-vertical drillholes, Y_2 should present high correlation with Y_1. Therefore, as Y_2 is exhaustively known, it will have a strong impact on the simulation of Y_1; in particular, it will force the realizations of Y_1 to 'adhere' to the interpretive geological model, as if this model (soft data) were as reliable as the drillhole data (hard data). This feature may be partly undesirable, and one may think of reducing the influence of the soft data on the outcomes of Y_1, from which the simulated geological models will be derived.

The proposed solution is to introduce a corrective scaling coefficient ρ, with a value between 0 and 1, which represents the level of confidence of the interpretive geological model, and to multiply the sill of the cross-covariance or cross-variogram between Y_1 and Y_2 by this coefficient. If $\rho = 1$, the previous coregionalization model is unchanged and the influence of Y_2 upon Y_1 is maximal, while if $\rho = 0$, Y_2 is uncorrelated with Y_1 and has no influence on the simulation of Y_1 any more (the simulation is conditioned only to the drillhole data). The best value of ρ can be chosen based on geological considerations or through cross-validation techniques, as it is illustrated below.

Joint Simulation of Y_1 and Y_2, Back-Transformation and Truncation

The two Gaussian random fields Y_1 and Y_2 are jointly simulated, e.g., with a spectral algorithm

(Emery et al., 2016), conditioned to the drillhole (hard) data and the interpretive model (soft data) and back-transformed to the original random fields Z_1 and Z_2. The unit indicator is finally obtained by truncating Z_1 at threshold 0, because the boundary of the target unit corresponds to the set of points where Z_1 is zero (the truncation of Z_2 coincides with the interpretive geological model, provided that Z_2 is known at each target node and its simulation reproduces the conditioning Z_2-data, so that it does not reflect any uncertainty, whereas the truncation of Z_1 varies from one realization to another at locations where there are no hard data).

The conditioning relies on a cokriging step (Chilès & Delfiner, 2012), which usually assumes that the two Gaussian random fields have a zero mean. To weaken this assumption and to allow the mean values of these fields to vary at a global scale, while being approximately constant at a local scale, we suggest to assume that the mean values (m_1 and m_2) are unknown and related as follows (Emery, 2012):

$$m_1 - t_1 = a(m_2 - t_2) \tag{2}$$

where t_1 and t_2 are the Gaussian equivalents of the zero distance, and $a = \text{cov}\{Y_1,Y_2\}/\text{var}\{Y_2\}$ is the slope of the regression of Y_1 (dependent variable, known only at the drillhole locations) upon Y_2 (independent variable, exhaustively known). This slope can be calculated based on the direct and cross-variograms of Y_1 and Y_2. Accordingly, when the local mean of Y_2 is equal to t_2, then the local mean of Y_1 is equal to t_1, i.e., the geological unit boundary determined from the soft data information ($Y_2 = t_2$) agrees with the boundary determined from the hard data information ($Y_1 = t_1$), which allows a better 'adherence' of the simulated units with the interpreted ones in areas with few hard data. Note that, the mean values m_1 and m_2 do not need to be specified; the conditioning cokriging assumes that they are constant at the scale of the cokriging neighborhood, but unknown, and can vary from one neighborhood to another while satisfying Eq. 2.

SYNTHETIC CASE STUDY

A synthetic case study was generated in order to assess the capability of the proposed approach for simulating non-stationary geological units in the presence of few drillhole data. To this end, an interpretive model corresponding to a two-dimensional vertical cross section with two units was generated with 58,118 nodes and a spacing of 2 × 2; 98 data forming seven drillholes were sampled from the interpretive model (Fig. 3). This synthetic case represents a porphyry-like body housed in a generic wall rock.

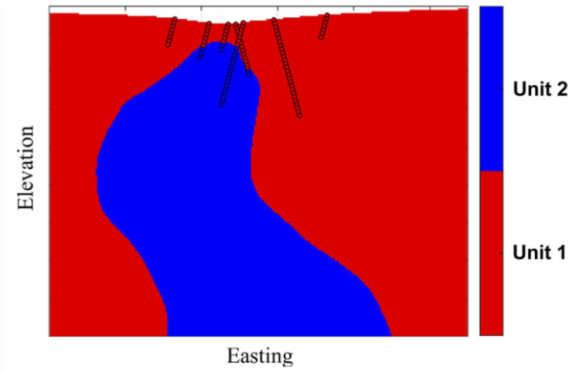

Figure 3. Interpretive geological model and drillhole data (synthetic case study). White nodes correspond to air.

The down-the-hole distance Z_1 was calculated for the 98 drillhole data, while the omnidirectional distance Z_2 was calculated for the 98 drillhole data and the 58,118 grid nodes. Then, both distances were transformed into Gaussian equivalents (Eq. 1), following the guidelines explained in section **Normal Scores Transformation** above, i.e., the vertical distance calculated for the 58,118 grid nodes was used to determine the normal scores transformation function of Z_1, based on the fact that the experimental transformation based on only 98 data lacks robustness. Figure 4 shows the histogram and the experimental and modeled direct and cross-variograms of the normal scores data. An isotropic model, consisting of a cubic structure with a range of 370, was assumed here, which yielded a good fit of the experimental variograms:

$$\begin{aligned}\Gamma(\boldsymbol{h}) &= \begin{pmatrix} \gamma_{11}(\boldsymbol{h}) & \gamma_{12}(\boldsymbol{h}) \\ \gamma_{12}(\boldsymbol{h}) & \gamma_{22}(\boldsymbol{h}) \end{pmatrix} \\ &= \begin{pmatrix} 0.91 & 0.81 \\ 0.81 & 0.74 \end{pmatrix} cubic_{370}(\boldsymbol{h}). \end{aligned} \tag{3}$$

Four different values of the ρ coefficient (1, 0.625, 0.375, 0) for downscaling the cross-variogram sill were considered to assess the influence of the interpretive model in the simulation results. The case $\rho = 1$ corresponded to the maximum confidence in the interpretive model and the maximum resem-

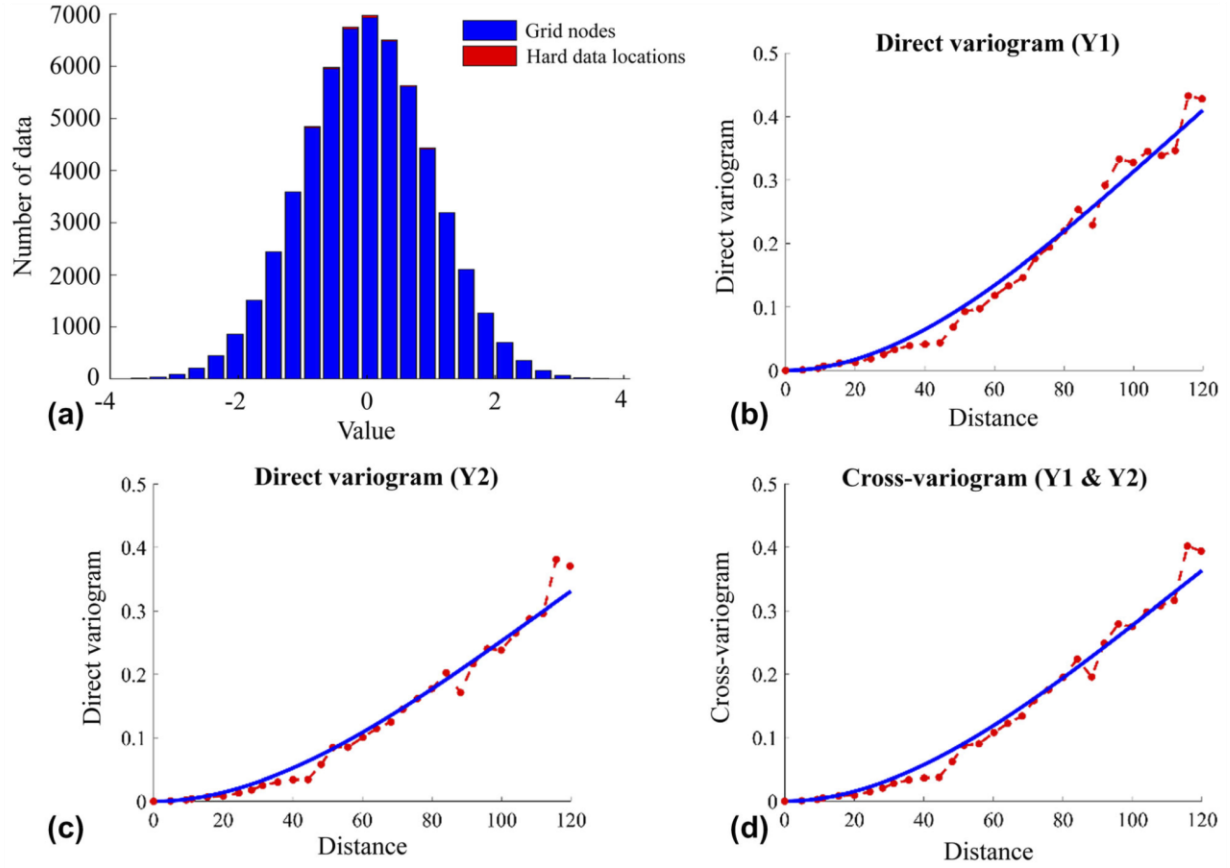

Figure 4. (**a**) Histogram of normal scores of soft data (Y_2) at the grid nodes and drillhole locations; the bars of the histogram are split into two colors to distinguish the grid nodes (blue) from the drillhole locations (red). (**b**), (**c**) and (**d**) Experimental (red) and theoretical (blue) direct and cross-variograms of Y_1 and Y_2. The variograms are shown for lag separation distances between 0 and 120, although the models have a correlation range of 370.

blance between this model and the simulated units (Fig. 5a, b), even in sectors with no drillhole data. As ρ decreased, the resemblance faded (Fig. 5c–f) until it disappeared when $\rho = 0$ (Fig. 5g, h). This situation is reflected in the probability maps obtained from a set of 100 realizations (Fig. 6). The case $\rho = 1$ provided probabilities mostly close to 0 or to 1, except for a tiny zone enclosing the unit boundary in the interpretive model, even in the deepest sector with no drillhole data. In contrast, the case $\rho = 0$ provided probabilities close to 0 or to 1 only in the neighborhood of the drillhole data (superficial sector).

It is concluded that although there exist no drillhole data in depth, the proposed approach was able to reproduce non-stationary features in accordance with the interpretive geological model, and thus allowed incorporation of geological knowledge in the geostatistical simulation. In addition, by introducing the coefficient ρ, one can modulate the influence of the interpretive model, from a complete confidence ($\rho = 1$) to no confidence at all ($\rho = 0$). Such a model partially compensates the lack of direct (hard) drillhole data.

Geological considerations can help to decide which value of ρ is the most suitable. The probability maps in Figure 6a, d are unrealistic because the first map lacked depth uncertainty (which is not possible if one only has information in superficial areas) and the last map illustrates a body that is not in accordance with a synthetic geological model of porphyry type. The maps in Figure 6b, c make more geological sense; however, the latter narrows the base of the porphyry body too much, which is unlikely. Thus, based on a geological (non-mathematical) criterion, one can choose the confidence coefficient $\rho = 0.625$

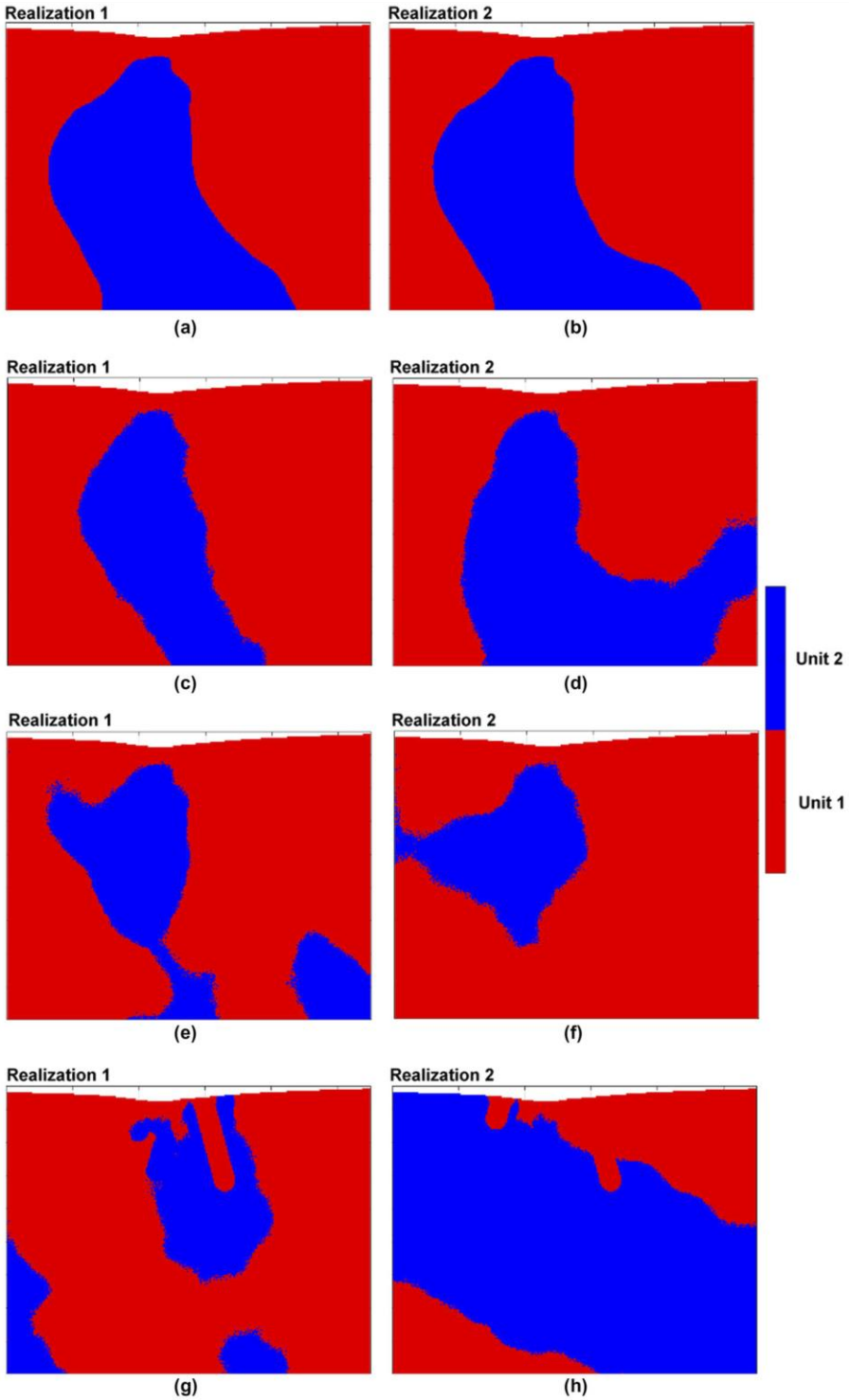

Figure 5. Two realizations of the geological units, obtained with $\rho = 1$ (**a**, **b**), $\rho = 0.625$ (**d**, **e**), $\rho = 0.375$ (**e**, **f**) and $\rho = 0$ (**g**, **h**).

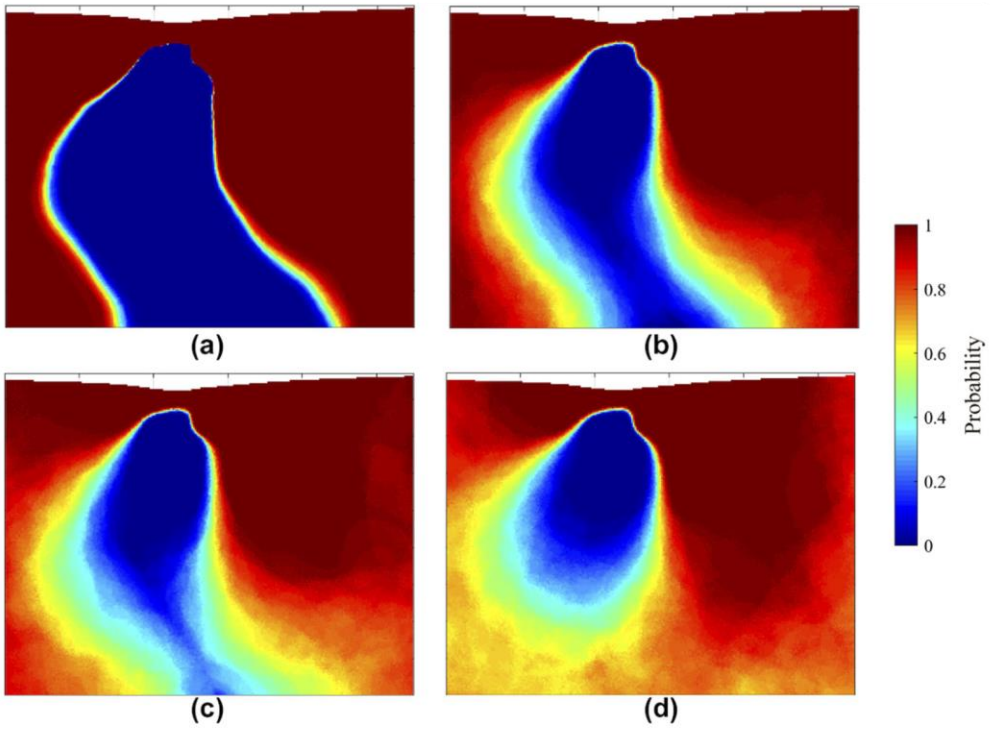

Figure 6. Probability of occurrence of unit 1 for $\rho = 1$ (**a**), $\rho = 0.625$ (**b**), $\rho = 0.375$ (**c**) and $\rho = 0$ (**d**).

in this particular example. In section **Choice of the Confidence Coefficient** below, we propose a more 'objective' method for selecting ρ, which can complement expert judgment.

REAL CASE STUDY: SPENCE PORPHYRY COPPER DEPOSIT

Geological Framework

The Spence copper mining and processing operation in northern Chile is owned by BHP Billiton. The fundamental description of the geological setting and nature of the Spence deposit was derived from geological field mapping and drillhole samples, including radiometric dating of a range of lithologies comprising intrusive porphyry bodies, and it is interpreted as a typical porphyry Cu deposit of the Atacama Desert with supergene enrichment. The deposit is located at 150 km NE from Antofagasta city, at an altitude of 1750 m above mean sea level, in the metallogenic Paleocene belt (Boric et al., 1990).

Lithology

The San Salvador and Quebrada Mala Formations (*JKiss-Ksqm*) are the main lithological units in the Spence district and, together with intrusive porphyry bodies, are the main host of Cu mineralization. They are composed of a well-stratified continental sedimentary succession formed by purple-colored, laminated siltstones, fine- to coarse-grained gray sandstones, conglomerate sandstones, supported matrix conglomerates in the bottom part, and rhyolitic and dacitic lavas and tuffs, porphyritic, banded, fluid light gray to burgundy tones, with few phenocrystals of quartz and plagioclase in a fundamental mass or vitreous matrix in the upper part (Duhart et al., 2018). These units are included in a single undifferentiated 'wall rock unit' of the lower to upper Cretaceous.

The deposit comprises three main intrusive porphyry centers arranged *en echelon* along a broadly NNE–SSW trend that comprises various intrusive pulses (*Pai(b1)*). These intrusive lithologies consist of granodiorite to quartz monzonite hypabyssal porphyries. The intrusives are Paleocene

in age, approximately 57 Ma (Bunker et al., 2017), and brecciation has overprinted the porphyry bodies during the later stages of their emplacement, in some cases associated with significant tourmaline developments. These intrusions were grouped in a 'quartz-felspathic porphyry unit' of the Paleocene.

Over the previous units lies a coverage of gravel deposits, sand and silt of colluvial and fluvial origin mainly, which are currently active from Pleistocene to Holocene (*PlHac*). Finally, anthropic deposits lie on the surface derived from the mining processes (*Han*). This geological setting is summarized in Figure 7.

Mineralization

The Spence Cu mineralization under gravel deposits comprises horizontal layers of leached cap, supergene oxide and secondary sulfide mineralized units, which extend at least 3600 m in the SSW–NNE direction and 1000 m in the E–W direction. The profile is typical of supergene-enriched porphyry Cu deposits and has resulted from a supergene Cu leaching and enrichment process that has subsequently undergone partial in situ oxidation. Underlying this supergene profile, the hypogene mineralization presents a much greater vertical extent to depth and is controlled by sub-vertical intrusive and breccia bodies (Moreno et al., 2012).

During 2020–2021, Spence began a process of ore concentration associated mainly with Cu sulfides present in the secondary, transitional and primary sulfide units, which, accounting for lithology and hydrothermal alteration, generate metallurgical units with different Cu recoveries. The uncertainty in the boundaries of these three mineralized units is the focus of this case study. The descriptions of the four mineralized units under consideration are as follows.

Supergene Unit (Leached Cap and Cu Oxides)

This unit is the grouping of the leach cap that comprises the interval in which Cu minerals have been leached out by natural processes with the presence of extensive iron oxides of various types. It does not present visible mineralization of Cu, and supergene oxide is characterized by the presence of atacamite, brochantite and chrysocolla with minor presence of secondary sulfides such as chalcocite.

Secondary Sulfide Unit (Predominant Chalcocite)

This mineralization resulted from physical and chemical changes to sulfides and silicates, which are termed 'supergene enrichment.' The predominant ore minerals in this secondary sulfide zone are chalcocite and minor covellite. These minerals partially or completely replace pyrite, chalcopyrite and covellite.

Transitional Sulfide Unit (Low Enrichment)

As depth increases, the proportion of chalcopyrite increases and chalcocite and covellite generally decrease and mark a transition between full secondary sulfides above (chalcocite + pyrite ± covellite) and full primary sulfides below (chalcopyrite + pyrite).

Primary Sulfide Unit (Hypogene with Predominant Chalcopyrite)

Hypogene mineralization is located at depth below secondary and transitional sulfides. It is characterized mainly by chalcopyrite + pyrite with minor presence of covellite and chalcocite. The hypogene Cu mineralization is controlled strongly by the volumetric distribution of the porphyry intrusive bodies and the subsequent hydrothermal alteration of these intrusive bodies.

Available Information

Figure 8 shows a cross section with drillhole information (about 140,000 hard data in the entire deposit, each data consisting of a core composite with length of 5 m and for which the prevailing mineralized unit has been logged) and the interpretive model (soft data). Based on the fact that the interpretation is subject to errors, our proposal accounts for the level of confidence on this interpretation in the definition of a confidence coefficient, as detailed in the next section.

In production plans, the volumes to be fed in the next periods have high density of information, but periods more distant in time do not. The latter have greater uncertainty because the boundaries of the mineralized units are delineated with less information, implying that the modeler must make an

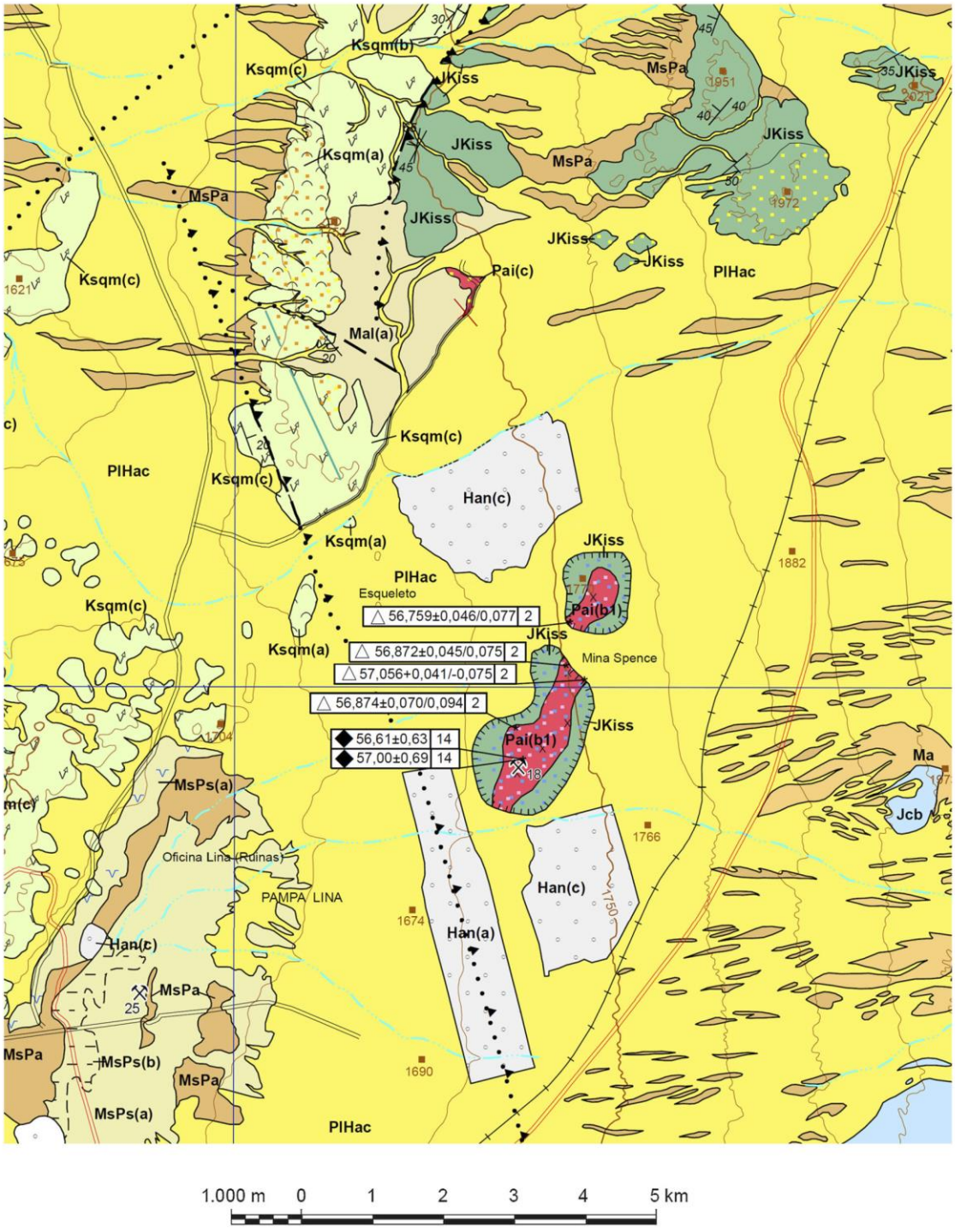

Figure 7. Geological map of Sierra Gorda, northern Chile, around the Spence mine (modified from Duhart et al., 2018). The main lithologic units are the wall rocks unit (*JKiss-Ksqm*), copper porphyries (*Pai(b1)*), alluvial and colluvial deposits (*PlHac*) and anthropic deposit (*Han*).

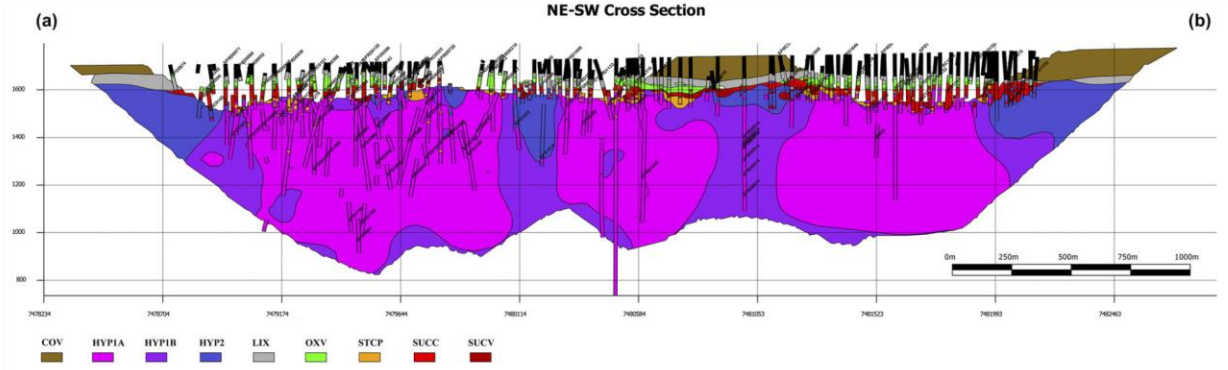

Figure 8. NE–SW cross section (interpretive model, with superimposed drillhole data) of the Spence mineralization. The main mineralized units are the cover (*cov*), supergene (*lix-oxv*), secondary sulfides (*succ-sucv*), transitional sulfides (*stcp*) and primary sulfides (*hyp1a-hyp1b-hyp2*).

interpretation based on his/her own expertise. What is the risk associated with generating long-term plans with this interpretation in distant volumes? This question commonly arises when analyzing uncertainty in production plans, and it can be answered by the application of conditional simulation.

HIERARCHICAL MODELING AND SPATIAL STRUCTURE IDENTIFICATION

Our proposal rests on the following hierarchical modeling:

- In the first step, the primary sulfide unit is simulated;
- The supergene unit is then simulated in the complement of the primary sulfide unit; and
- The secondary and transitional sulfide units are finally simulated in the complement of the first two units.

Because the interpretive model contains many nodes, the amount of data from the second variable (Z_2, omnidirectional distance to the boundary) is significantly more than the number of data from the first variable (Z_1, down-the-hole distance to the boundary). Accordingly, after transforming these variables into Gaussian equivalents (Y_1 and Y_2) (Eq. 1), a joint variogram analysis is performed by using only the normal scores at the drillhole locations. This restriction aims to avoid inconsistencies between the experimental direct and cross-variograms, e.g., violations of Cauchy–Schwarz's inequality (Wackernagel, 2003), but it leads to direct variograms with sills much lower than the expected unit sill (Fig. 9), the reason being that the drillhole data are mostly clustered in the center and top of the deposit and do not reflect the whole range of signed distances calculated from the interpretive model (Fig. 10). The latter inconvenience is solved by rescaling the direct and cross-variograms of Y_1 and Y_2 as follows:

$$\tilde{\Gamma}(\boldsymbol{h}) = \begin{pmatrix} \tilde{\gamma}_{11}(\boldsymbol{h}) & \tilde{\gamma}_{12}(\boldsymbol{h}) \\ \tilde{\gamma}_{12}(\boldsymbol{h}) & \tilde{\gamma}_{22}(\boldsymbol{h}) \end{pmatrix} = \begin{pmatrix} \frac{\gamma_{11}(\boldsymbol{h})}{\gamma_{11}(\infty)} & \frac{\gamma_{12}(\boldsymbol{h})}{\sqrt{\gamma_{11}(\infty)\gamma_{22}(\infty)}} \\ \frac{\gamma_{12}(\boldsymbol{h})}{\sqrt{\gamma_{11}(\infty)\gamma_{22}(\infty)}} & \frac{\gamma_{22}(\boldsymbol{h})}{\gamma_{22}(\infty)} \end{pmatrix}, \quad (4)$$

where γ_{ij} $(i, j = 1, 2)$ are the non-rescaled variograms, $\gamma_{ij}(\infty)$ are their sills and $\tilde{\gamma}_{ij}$ are the rescaled variograms, ensuring a unit sill (unit variance) for the two Gaussian random fields Y_1 and Y_2. As the sampling design (clustered in the top and center of the deposit) can affect the calculation of experimental variograms, especially along the vertical direction, only omnidirectional variograms were considered and fitted with isotropic models, all the more so because no anisotropy could be identified at small lag separation distances.

Choice of Confidence Coefficient ρ

The last parameter needed for simulating the mineralized units is the coefficient ρ introduced to downscale the cross-variogram between Y_1 and Y_2. To this end, a cross-validation was performed with

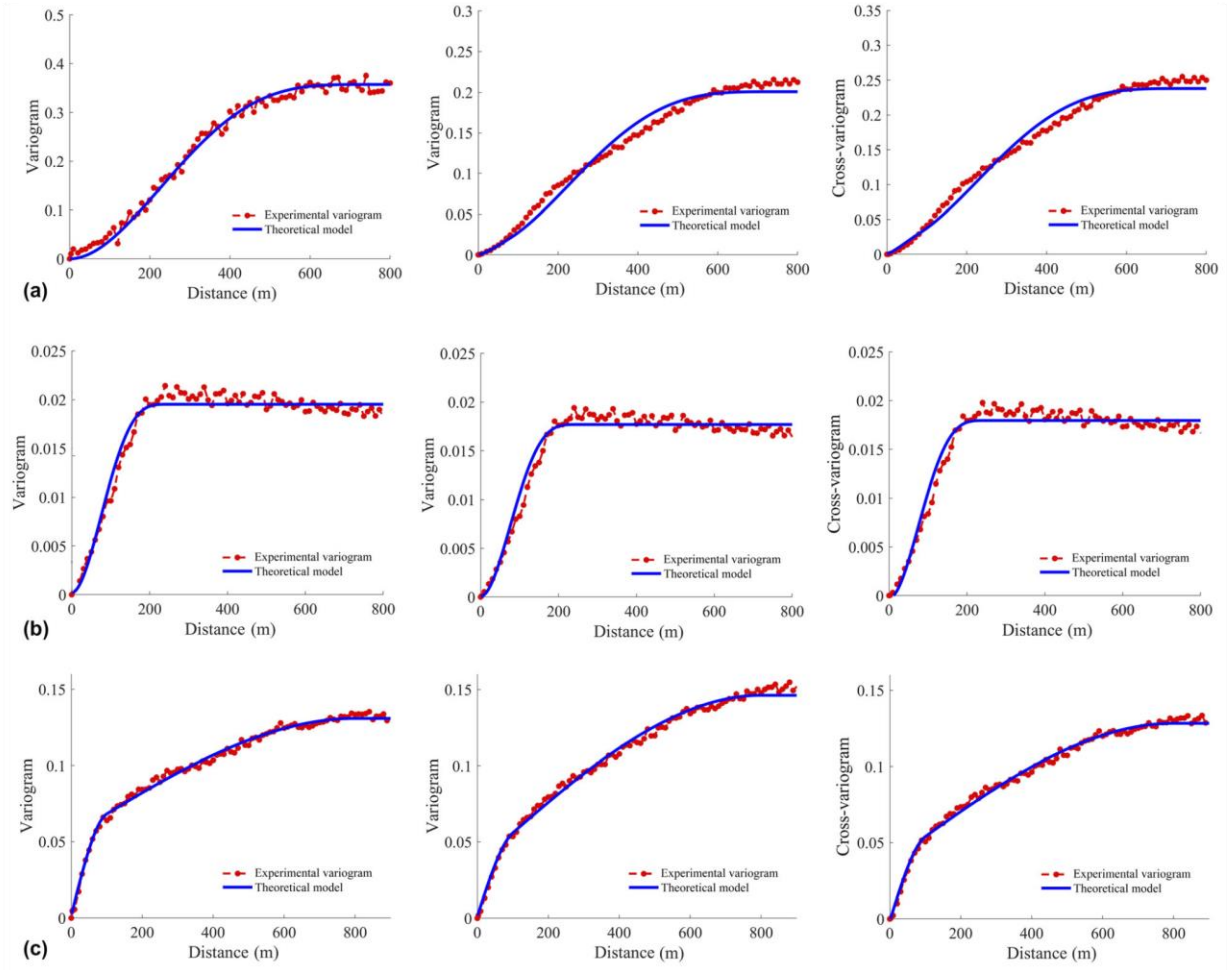

Figure 9. Experimental (dash lines) and theoretical (solid lines) direct and cross-variograms of Y_1 and Y_2 for (**a**) step 1, (**b**) step 2 and (**c**) step 3 of the hierarchical modeling. The theoretical models consist of isotropic combinations of cubic and spherical structures. Left panels: direct variograms of Y_1. Middle panels: direct variogram of Y_2. Right panels: cross-variogram between Y_1 and Y_2.

different values of ρ. In detail, at each drillhole data location, one hundred realizations of the mineralized units were constructed, conditionally to the interpretive model and to the other drillhole data located between 100 and 500 m from the target drillhole data, and then, the probability of occurrence of each unit was calculated. The minimum distance of 100 m was chosen in order to leave out the immediate neighbors in the same drillhole as the target data, which have a (too) large influence on the simulation.

For a given probability p (up to some calculation tolerances), it is expected that a proportion p of the drillhole data actually matches the underlying mineralized unit (Madani & Emery, 2015). For instance, one expects that half of the data having a probability of occurrence of the supergene unit equal to 50% truly belong to this unit. The comparison of the probability of occurrence and the data proportion can be made for any probability p and any mineralized unit and sensitized with the value of ρ input in the simulation algorithm.

Figure 11 shows the results obtained for the supergene unit in the second level of the binary tree: When ρ was greater than 0.8, the model lost accuracy (the mismatch between the probabilities of occurrence and data proportions increased), which suggests the value $\rho = 0.8$ as the one that led to an accurate simulation model and, at the same time, that made the simulated supergene unit adhere to the interpretive geological model in areas with no or few drillhole data. The same value 0.8 was also

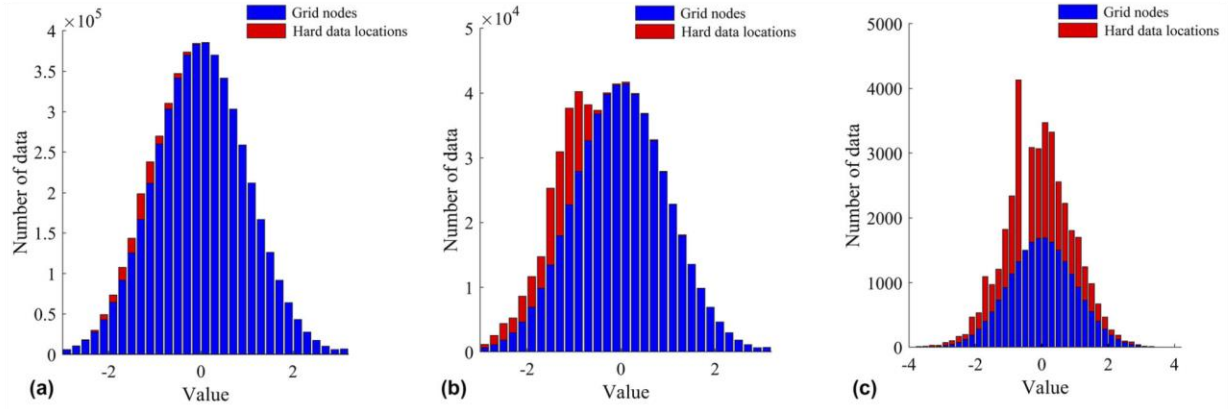

Figure 10. Histograms of the soft data Gaussian equivalent Y_2, at the grid nodes of the interpretive model and at the drillhole locations, for (**a**) step 1, (**b**) step 2 and (**c**) step 3 of the hierarchical modeling. The bars of the histograms are split into two colors to distinguish the grid nodes (blue) from the drillhole locations (red). The drillholes are scarce in the peripheral areas and in depth and are not representative of the entire deposit.

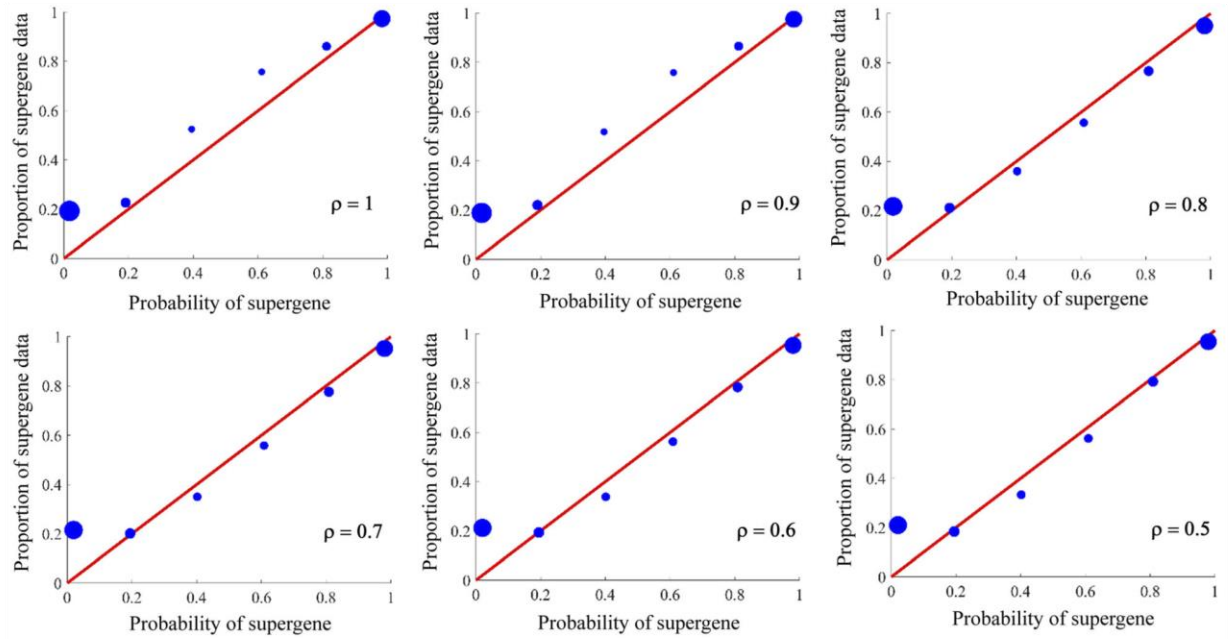

Figure 11. Cross-validation for confidence coefficients ρ ranging between 1 and 0.5. Comparison of the probability of occurrence of the supergene unit (horizontal axis) with the proportion of data that actually belong to the supergene unit (vertical axis). Dot size in the plot is proportional to the number of data involved.

found for the other levels of the binary tree for simulating the primary, secondary and transitional sulfide units.

One notes a slight mismatch for the first point in the plots of Figure 11. Among the drillhole data with probability (according to the simulation results) close to zero of being supergene, the true proportion of supergene data was about 20%. Such a mismatch may not be due to failure of the geostatistical model or the simulation algorithm, but to inconsistencies between the hard and soft data. Some drillhole data were logged as supergene but, in the interpretive model, belong to another unit (mainly, the primary sulfide) (Table 1). Hence, in the first step of the

Table 1. Confusion matrix contrasting the mineralized unit logged in the drillhole data with respect to the interpretive unit at the data locations. About 5% of the data do not agree with the interpretive model

	Interpretive geological model			
	Primary sulfide	Supergene	Secondary sulfide	Transitional sulfide
Drillholes				
Primary sulfide	57,542	188	623	860
Supergene	192	60,037	813	84
Secondary sulfide	744	725	10,694	461
Transitional sulfide	997	60	666	4398

hierarchical simulation that considers the interpretive model as a covariate, these data tended to be simulated as primary sulfide, even when setting ρ to 0.5, and their probability of being supergene was therefore close to zero.

The above inconsistencies were not always due to a mis-log of the hard data or a misinterpretation of the soft data, because they may be explained by interpolation errors when every drillhole data were assigned the mineralized unit of the nearest grid cell in the interpretive model. It even happened that a grid cell contained several drillhole data (e.g., consecutive composites of a same drillhole) with different logs, so that interpolation errors were unavoidable. One solution would be to re-log the drillhole data in accordance with the geological interpretation, but this would make the latter be considered as ground truth, while it was actually not 100% trustworthy. As a further matter, the fact that the interpretive model did not always match the hard data can be a desirable property, because geologists and metallurgists are not interested in isolated occurrences of a mineralized unit (for instance, a supergene data immersed in the primary sulfide unit, or vice versa), and they prefer to work on an 'operative' geological model that filters out variations at very short scales.

Simulation of Mineralized Units

After determining the joint spatial structure and setting the value of the ρ coefficient, one hundred conditional realizations of Y_1 and Y_2 were generated on a grid with a mesh of 20 m $\times$ 20 m $\times$ 15 m (the same as that of the interpretive model), providing, after back-transformation and truncation, one hundred realizations of the mineralized units. To reduce the computational burden, a moving neighborhood with a radius of 500 m was considered to search the primary (drillhole) and the secondary (interpretive model) data in the conditioning stage.

Figure 12 shows a plan view of the drillhole data, interpretive model, first realization and the most probable unit at each grid node, calculated on the basis of 100 realizations. The latter view turned out to be similar to the interpretive geological model, which arose because the chosen confidence coefficients ($\rho = 0.8$ in all the levels of the binary tree) entailed a pretty high confidence in this interpretive model. In contrast, the unit boundaries in an individual realization (Fig. 12a) deviated more from the interpretive model, reflecting the geological uncertainty. Noticeably, in the central area where drillhole data were abundant and the four mineralized units coexist, the realizations exhibited more variations than in peripheral areas, which can be explained because of the short-scale variability of the conditioning drillhole data in this central area. It is not uncommon that the unit logged at a data location differed from the one logged at a data from an adjacent drillhole situated 20–40 m away (roughly once or twice the grid mesh). In addition, the examination of consecutive data along a same drillhole showed that at this particular elevation, the mineralized units were sometimes intermingled at the scale of a few meters. This short-scale variability, together with the fact that the simulation was carried out on a relatively coarse grid, made the realizations less smooth in the central area of the chosen plan view in comparison with the borders or to other plan views where the transitional and secondary sulfide units were absent and the supergene and/or primary sulfide units were prevalent.

The maps in Figure 12 can be complemented by the maps of the probability of occurrence of each unit at each target grid node (Fig. 13), calculated based on the realizations, which provide a measure

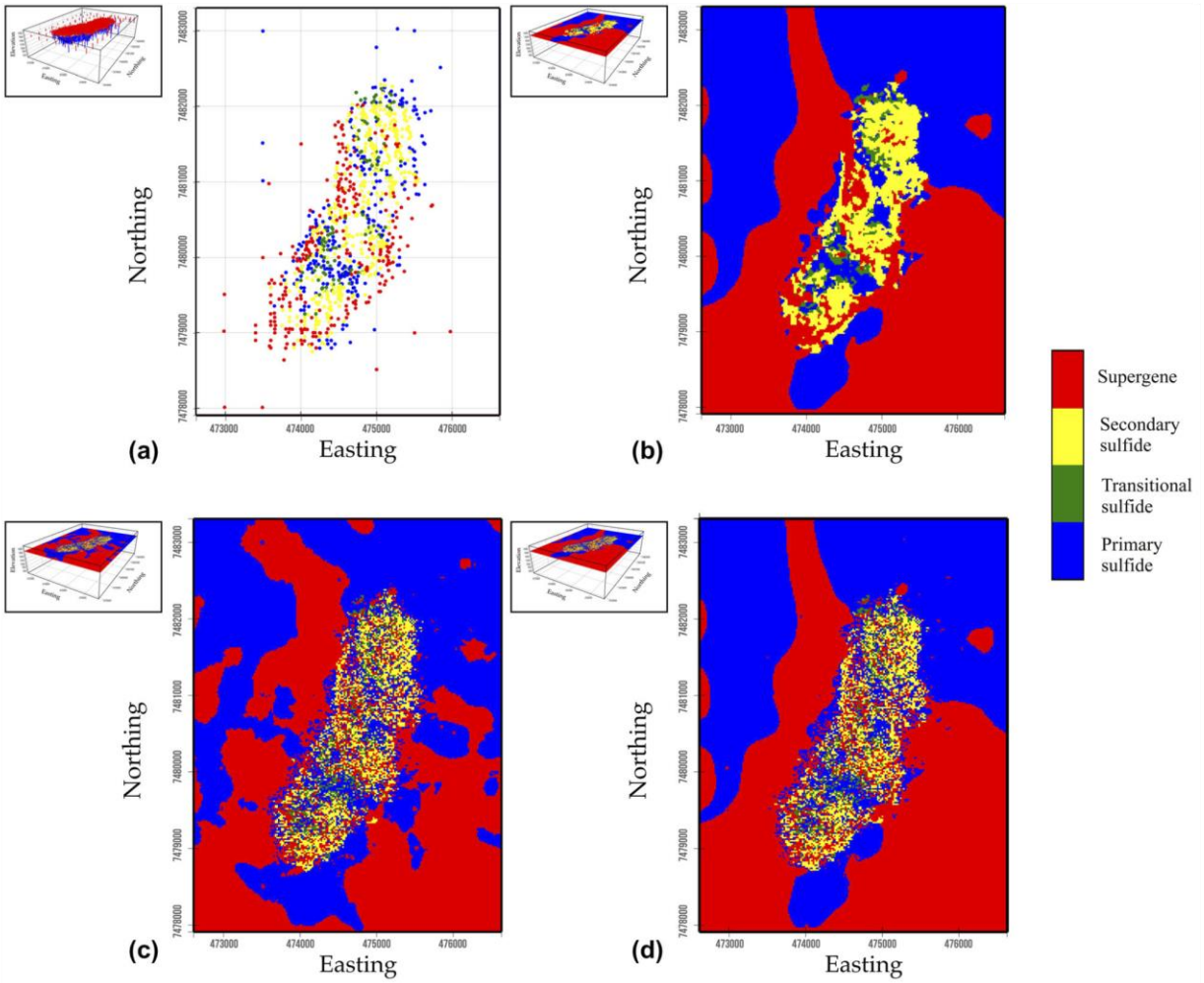

Figure 12. (**a**) Plan view of the drillhole data. (**b**) Interpretive geological model. (**c**) First realization obtained with the proposed implicit boundary simulation approach. (**d**) Most probable mineralized unit calculated from 100 realizations.

of how likely are the predictions in Figure 12b (interpretive model) or in Figure 12d (most probable unit) to be mistaken. In the central part of the maps, where the drillhole data were abundant, the probabilities were often close to zero or to one, indicating little geological uncertainty, whereas the probabilities had a wider spread in the peripheral parts where drillholes were scarce.

Comparison with Sequential Indicator Simulation

We ended this case study by comparing the results of implicit boundary simulation with those of an explicit approach, namely sequential indicator simulation (Alabert, 1987). The same hierarchical workflow was applied, whereby at each step, a mineralized unit was simulated at the grid nodes that were assigned any unit in the previous steps. Here, the model relied on the mean value and direct variogram of the target unit indicator. The latter was fitted with an isotropic model (Fig. 14, left side), while the former was identified with a moving average of the interpretive geological model indicator, with a moving window of 500 m of radius in the horizontal plane and 100 m in the vertical direction. This way, the probabilities of occurrence of the units varied in space in accordance with the

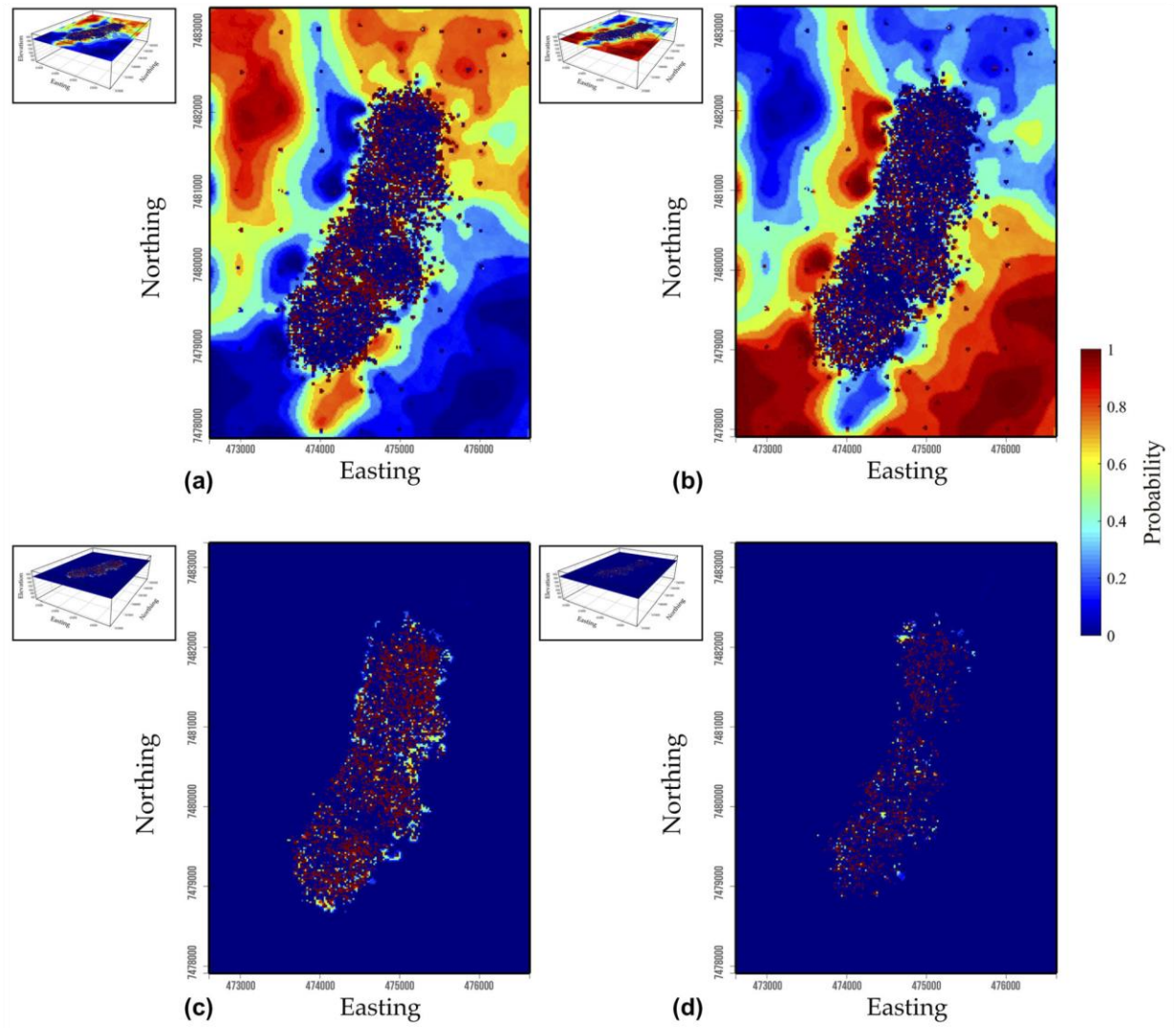

Figure 13. Probability maps estimated from 100 realizations: (**a**) primary sulfide; (**b**) supergene unit; (**c**) secondary sulfide; and (**d**) transitional sulfide.

geological interpretation, which allowed the realizations to adhere to this interpretation (Deutsch, 2006). Unlike implicit boundary simulation, the workflow was essentially univariate: one only simulates indicator values constrained with primary drillhole data, with no secondary data; the interpretive model is accounted for through the local mean of the indicators.

Two realizations are displayed in Figure 14 (right side), together with the most probable unit obtained over 100 realizations. The differences with implicit simulation are striking: (i) the boundary between the primary sulfide and supergene units was much more irregular than what would be expected from the linear growth of the primary sulfide indicator variogram near the origin (Emery & Lantuéjoul, 2011); (ii) the transitional sulfide was scattered over all the plan view, instead of only in the central part where its probability was nonzero (this can be explained because, even if one sets the indicator mean value to zero, indicator kriging may still provide a prediction greater than zero); (iii) the map of the most probable unit (Fig. 14f) bore less resemblance to the interpretive model; more resemblance

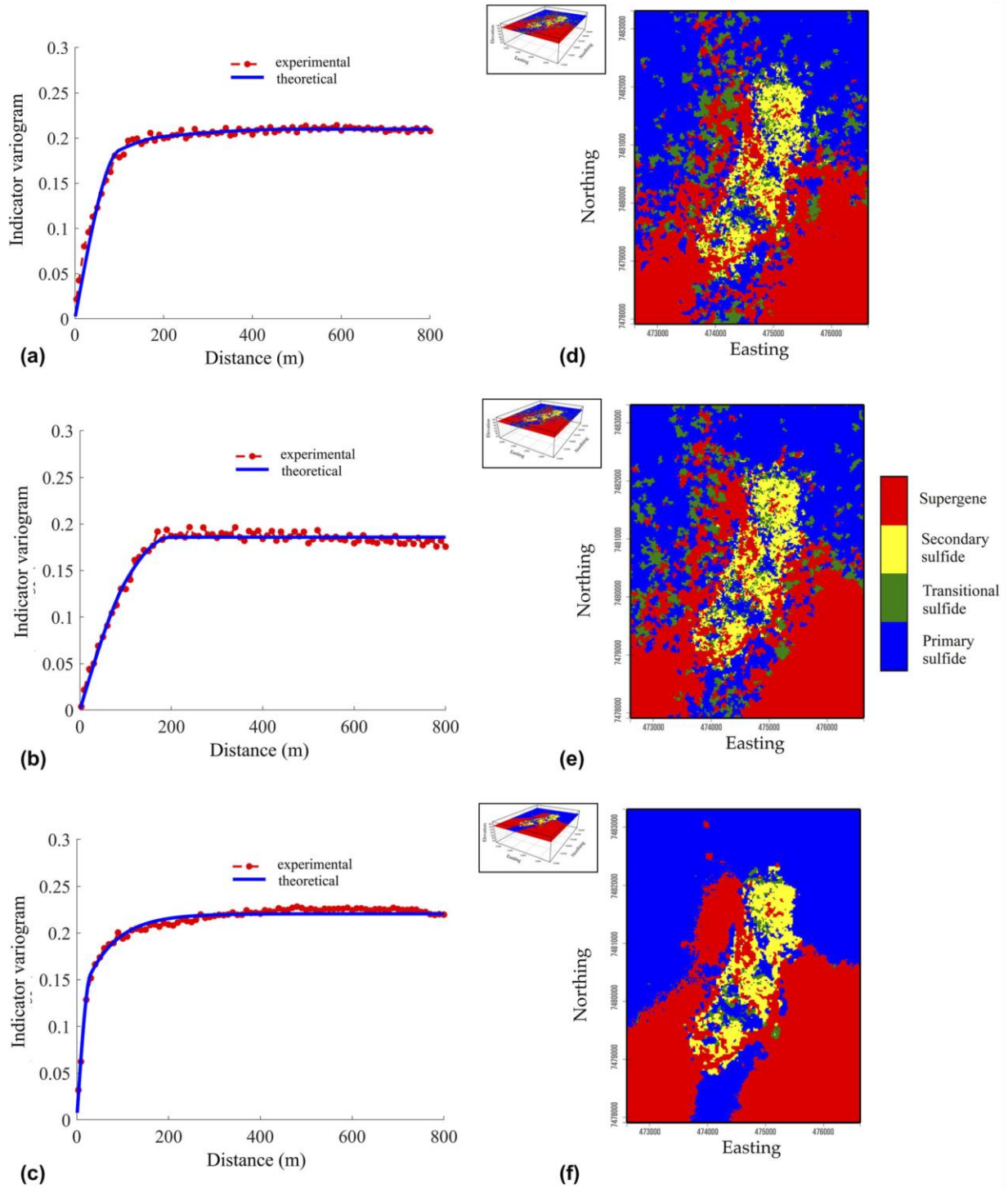

Figure 14. Experimental (dashed lines) and theoretical (solid lines) indicator variograms for (**a**) step 1, (**b**) step 2 and (**c**) step 3 of the hierarchical modeling. The theoretical variograms consist of combinations of isotropic spherical and exponential structures. (**d**) and (**e**) Plan views of two realizations obtained with sequential indicator simulation. (**f**) Most probable mineralized unit calculated from 100 realizations.

could be obtained by reducing the size of the moving window used to calculate the local mean values, at the price of smaller fluctuations across the realizations (Madani & Emery, 2015). In particular, the above statements (i) and (ii) show that even in areas with few hard data, sequential indicator simulation failed to reproduce the model parameters (indicator means and variograms), which was due to the fact that indicator kriging weights are not always contained in the [0,1] interval (Emery, 2004).

DISCUSSION

Modeling Assumptions

Implicit boundary models rely on the definition of a signed distance between any target location and the closest unit boundary, either along the drillhole direction (down-the-hole distance) or over all the directions (omnidirectional distance). One can be surprised by the decision to represent this kind of variable by the transform of a Gaussian random field and by the use of geostatistical simulation techniques to interpolate this variable in space, because the signed distance exhibits a systematic pattern of spatial variations. That is, at any location, it has a unit gradient in the direction joining this location to the closest boundary, which does not really fit with random variations and with a Gaussian random field representation. The success of the approach can be explained because one does not actually require a perfect modeling of the signed distance, but only of whether or not this distance is positive (geological unit of interest) or negative (complementary unit), i.e., what really matters is the modeling of the small distances (close to zero) rather than the whole distribution of distances.

Following the above argument, out of the parameters required to apply the proposed method, the most important are (a) the choice of the binary tree, which controls the topological relationships between geological units, (b) the spatial joint correlation structure of the normal scores data, which controls the spatial continuity of the simulated units, (c) the regularity of their boundaries and how the hard and soft conditioning data constrain the realizations, and (d) the corrective coefficient ρ, which controls the trustworthiness given to the soft data. A poor choice or a misspecification of these parameters is likely to significantly impact the simulation. In contrast, modeling of normal scores transformation functions (Eq. 1) really matters for signed distances close to zero, and the way that the tails of the signed distance distributions are transformed or back-transformed is not so relevant. As shown in the case studies, the quality of the simulation can be assessed visually to make sure that the realizations are geologically meaningful, and/or by cross-validation, to make sure that the realizations reproduce accurately the geological uncertainty.

Search Strategy

The fact that the levels of knowledge of the two signed distance variables are unbalanced (few Y_1 data vs. many Y_2 data) poses some implementation problems, in particular, in what refers to the selection of the relevant conditioning data. To circumvent these problems, in both case studies, a two-part search strategy was used to select the conditioning data. That is, one separately searches for neighboring drillhole data (with information of both the primary and secondary variables Y_1 and Y_2) and for neighboring data in the interpretive geological model (with information of Y_2 only). This way, one makes sure to select primary conditioning data, and all primary data are collocated with a secondary data. Such a strategy combines the multiple and multi-collocated search strategies recommended by Madani and Emery (2019), and it provides more accurate results in comparison with a strictly collocated search, where only the secondary data collocated with the target node are selected, even under a Markov approximation (Madani & Emery, 2019; Rivoirard, 2001).

Other Implementation Issues

One implementation aspect that causes difficulty is the definition of the signed distances for the data of a drillhole that does not intersect the unit boundary, i.e., the drillhole entirely belongs to a single unit (this situation happens for peripheral drillholes of shorter lengths in the supergene unit, see Fig. 8). Following the arguments in section **Modeling Assumptions** above, one just has to care for whether or not this distance can be close to zero. That is, for data located far from the drillhole end point, the distance to the boundary is large and, although its exact value is unknown, it can be set to an arbitrarily large value, without any significant impact

on the simulated unit boundary that corresponds to the zero distance. In contrast, for the data close to the drillhole end point, the distance to the boundary may be small (if the drillhole would have been a little deeper, it may have crossed the boundary), so the better option in this case is to let the down-the-hole distance remain unknown and to ignore the data in subsequent modeling and simulation stages. This was done in the real case study for data distance less than 50 m from the bottom end point of a drillhole.

A similar issue arising with the hierarchical workflow is the fact that once a unit is simulated, the down-the-hole distance may not be perfectly defined in the next levels of the binary tree. For instance, consider the tree in Figure 1. When unit 1 and its complement are simulated, it is possible that a piece of unit 1 separates drillhole data belonging to unit 2 from other data belonging to units 3 and 4, so only an upper bound of the down-the-hole distance can be calculated for the data at the second level. In other words, one actually calculates a pseudo-down-the-hole distance, which converts the drillhole data into an inequality constraint, the true distance being less than the calculated pseudo-distance. Accounting for such inequality data is feasible by recourse to iterative algorithms (Armstrong et al., 2011; Cáceres et al., 2011), but it is cumbersome and it increases the computational complexity of the simulation process. In the presented real case study, this problem was bypassed by the choice of the binary tree. That is, the first level simulated the primary sulfide unit located at depth, which did not separate any of the other three units; the second level simulated the supergene unit located near the surface, and this unit did not separate the two remaining units (secondary and transitional sulfide units), which were simulated in the third level.

Incorporation of Geological Knowledge

A geological model is a reference model built from the same data as the ones that will be input to the simulation, but with construction criteria subject to the experience of a professional who must generate a logical, sensible and conceptually accepted interpretation that is able to reproduce the genetic model of a deposit and which must also be predictive with new information. The traditional way to incorporate a geological interpretation into implicit boundary simulation is to consider that the Gaussian random field Y_1 is not stationary, but has a spatially varying mean value that depends on the interpretive geological model (Henrion et al., 2010). This stratagem makes the simulated units adhere to the interpretive model but it lacks theoretical foundations, in particular because the normal scores transformation and the variogram analysis are based on a stationarity assumption. In our proposal, the interpretive model is introduced by means of a covariate instead of a spatially varying mean value, which allows one not to depart from the stationarity assumption. At the same time, the introduction of the confidence coefficient ρ allows accounting for the fact that both hard and soft data cannot be used together as if they were equally reliable. That is, the problem is formulated as a joint simulation of two data sources that have different qualities, although they represent the same phenomenon, giving the geological interpretation a significant influence only in areas with little or no drilling information. Despite the stationarity assumption, it is seen that realizations can reproduce non-stationary features, such as geological zonations and trends (e.g., supergene unit near the surface and primary sulfide unit in depth), because the interpretive model is used to define the covariate (Y_2) that conditions the simulation of the main variable (Y_1). In some way, the soft conditioning data impose their local structure over the prior stationary model, see discussion in Journel and Huijbregts (1978), Journel and Rossi (1989), Emery and Robles (2009) or Maleki-Tehrani et al. (2013).

Need for Line-Segment Primary Data

The proposed approach is applicable when the primary data originate from drillholes or boreholes, for which it is possible to calculate the down-the-hole distance to the closest geological boundary. If the primary data were scattered in space, then it would not be possible to define such a distance unambiguously. Instead, one would calculate a pseudo-distance that represents an upper bound of the true distance to the boundary (Manchuk & Deutsch, 2019; also recall sections **Shortest Down-the-Hole and Omnidirectional Distances to Unit Boundary** and **Other Implementation Issues** above) and that could change when new primary data become available. This inconvenience is the reason why the primary variable is not the omnidirectional

distance to the closest boundary, as is the secondary variable.

Perspective for Improved Modeling

Some authors suggest the use of a non-Euclidean distance to unit boundary, which can account for global or local anisotropies (Henrion et al., 2010) and, therefore, is more informative than the down-the-hole distance. However, this does not solve a fundamental issue related to the definition of this variable, which is its directional-dependence. Indeed, the down-the-hole distance loses directional information and, provided that the drillhole orientations are ignored, is supposed to be approximately the same when a reference normal scores transformation function is considered, see section **Normal Scores Transformation** above. Following the work of Sánchez et al. (2019), one solution would be to regionalize the two distance fields Z_1 and Z_2 in a five-dimensional space consisting of the 3D Euclidean space (geographical space) crossed with a 2D sphere (directional space), so that these fields would be assigned five coordinates. On the one hand, the easting, northing and elevation of the drillhole data or of the grid node under consideration; on the other hand, the azimuth and dip along which the distance is calculated.

Another improvement of the method would consist in considering a spatially varying confidence coefficient $\rho(\mathbf{x})$, with $\mathbf{x}$ the spatial coordinate, instead of a constant coefficient ρ. The rationale is that the confidence in the interpretive geological model is not the same throughout a deposit and it makes sense to assume that modeling close to drillhole data has a higher level of confidence than away from these data. The reasons for not having developed such a solution are twofold. The first one relates to the inference stage: the confidence coefficient $\rho(\mathbf{x})$ should not only depend on the distance to the drillhole data, mainly a function of the easting and northing coordinates, but also on the elevation (for instance, in the real case study, one is more confident to find the supergene unit close to the surface and the primary sulfide in depth, the lowest confidence being at intermediate elevations where any of the four units can be found), and it is not clear how the horizontal and vertical variations of $\rho(\mathbf{x})$ could be defined in an objective manner. The second reason relates to mathematical restrictions, as not any spatially varying function $\rho(\mathbf{x})$ can be used to downscale the cross-variogram between Y_1 and Y_2. For instance, suppose that Y_1 and Y_2 have regular spatial variations (i.e., their direct variograms exhibit a smooth short-scale behavior) and are also strongly cross-correlated, and consider two neighboring locations $\mathbf{x}$ and $\mathbf{x}'$. If one sets $\rho(\mathbf{x})$ to 1, then the four random variables $Y_1(\mathbf{x}')$, $Y_1(\mathbf{x})$, $Y_2(\mathbf{x})$ and $Y_2(\mathbf{x}')$ will be strongly correlated, which prevents setting $\rho(\mathbf{x}')$ to 0, as this would make $Y_1(\mathbf{x}')$ and $Y_2(\mathbf{x}')$ being uncorrelated. Therefore, the choice of the spatially varying function $\rho(\mathbf{x})$ is not free and the conditions to get a mathematically valid model are largely unknown.

CONCLUSIONS AND PERSPECTIVES

An adaptation of implicit boundary simulation was proposed to account for two sources of information when simulating geological units in the subsurface: hard information originating from drillhole data and soft information from an interpretive geological model of the subsurface. The latter is introduced as a covariate that is cross-correlated with the primary variable associated with the former. By downscaling the cross-variogram between both variables, one can control the level of confidence of the soft information. A downscaling coefficient equal to 1 yields the maximum resemblance between the interpretive model and the simulated geological units, while a coefficient equal to 0 makes the interpretive model to have no influence on the simulation. The choice of such a coefficient can be guided by geological considerations and/or by cross-validation techniques.

The proposed algorithm was applied in two case studies, one synthetic and one corresponding to a porphyry Cu deposit. In both cases, the simulated units reproduce the spatial zonation of the interpretive geological model. The implementation has revealed difficulties related to the calculation of the down-the-hole distance to unit boundary, normal scores transformation, variogram analysis and consistency between hard and soft information. As perspectives for future work, one can imagine that the coefficient used to quantify the confidence in the interpretive geological model may vary in space, or that the data should be regionalized in a five-dimensional space in order to account not only for their geographical positions but also for the direction along which distances to unit boundaries are calculated.

ACKNOWLEDGMENTS

This research was partially supported by the National Agency for Research and Development of Chile (ANID), under Grant ANID PIA AFB180004 (R.F., X.E. and F.N.) and by BHP where the case studies were conducted. The authors acknowledge two anonymous reviewers for their constructive comments.

REFERENCES

Alabert, F. (1987). Stochastic imaging of spatial distributions using hard and soft information. MSc. dissertation, Stanford University.

Amarante, F. A. N., Rolo, R. M., & Coimbra Leite Costa, J. F. (2021). Boundary simulation-a hierarchical approach for multiple categories. *Applied Earth Science: Transactions of the Institute of Mining and Metallurgy, 130*(2), 114–130.

Armstrong, M., Galli, A., Beucher, H., Loc'h, G., Renard, D., Doligez, B., Eschard, R., & Geffroy, F. (2011). *Plurigaussian simulations in geosciences*. Springer.

Aug, C., Chilès, J. P., Courrioux, G., & Lajaunie, C. (2005). 3D geological modelling and uncertainty: The potential-field method. In O. Leuangthong & C. V. Deutsch (Eds.), *Geostatistics Banff 2004* (pp. 145–154). Springer.

Benito Garcia-Morales, M., Beucher, H., Geffroy, F., & Doligez, B. (2003). Object-based simulations in fluvial environment at the reservoir scale and at a local scale. In: Proceedings of the AAPG annual convention. Salt Lake City, Utah. AAPG Search and Discovery Article #90013, 7 p.

Berry, M., & McCarthy, P. (2006). Practical consequences of geological uncertainty. In: Proceedings of the 6th international mining geology conference (pp. 253–258). The Australasian Institute of Mining and Metallurgy.

Beucher, H., Galli, A., Le Loch, G., & Ravenne, C. (1993). Including a regional trend in reservoir modelling using the truncated Gaussian method. In A. Soares (Ed.), *Geostatistics Tróia'92* (pp. 555–566). Springer.

Beucher, H., García-Morales, M., & Geffroy, F. (2005). Fitting the Boolean parameters in a non-stationary case. In O. Leuangthong & C. V. Deutsch (Eds.), *Geostatistics Banff 2004* (pp. 569–578). Springer.

Boric, R., Díaz, F., & Maksaev, V. (1990). Geología y yacimientos metalíferos de la Región de Antofagasta. Servicio Nacional de Geología y Minería, Boletín No. 40, 246 p.

Bunker, E., Blundy, J., Cooper, F., Condon, D., & Tapster, S. (2017). Textural, spatial and temporal variation within the igneous suites of the Spence porphyry copper deposit, northern Chile. *Applied Earth Science, 126*(2), 47–48.

Cáceres, A., Emery, X., Aedo, L., & Gálvez, O. (2011). Stochastic geological modeling using implicit boundary simulation. In J. Beniscelli, R. Kuyvenhoven, & K. O. Hoal (Eds.), *Proceedings of the 2nd international seminar on geology for the mining industry.* Gecamin Ltd.

Calcagno, P., Chilès, J. P., Courrioux, G., & Guillen, A. (2008). Geological modelling from field data and geological knowledge. Part I. Modelling method coupling 3D potential-field interpolation and geological rules. *Physics of the Earth and Planetary Interiors, 171*, 147–157.

Carle, S. F., & Fogg, G. E. (1997). Modeling spatial variability with one and multidimensional continuous-lag Markov chains. *Mathematical Geology, 29*(7), 891–918.

Carle, S. F., & Fogg, G. E. (2020). Integration of soft data into geostatistical simulation of categorical variables. *Frontiers in Earth Science, 8*, 449.

Carr, J. C., Beatson, R. K., Cherrie, J. B., Mitchell, T. J., Fright, W. R., McCallum, B. C., & Evans, T. R. (2001). Reconstruction and representation of 3D objects with radial basis functions. In L. Pocock (Ed.), *Proceedings of the 28th annual conference on computer graphics and interactive techniques* (pp. 67–76). Association for Computing Machinery.

Caumon, G., Gray, G., Antoine, C., & Titeux, M. O. (2013). Three-dimensional implicit stratigraphic model building from remote sensing data on tetrahedral meshes: Theory and application to a regional model of La Popa Basin, NE Mexico. *IEEE Transactions on Geoscience and Remote Sensing, 51*(3), 1613–1621.

Chilès, J. P., Aug, C., Guillen, A., & Lees, T. (2004). Modelling the geometry of geological units and its uncertainty in 3D from structural data: The potential-field method. In R. Dimitrakopoulos & S. Ramazan (Eds.), *Orebody modelling and strategic mine planning* (pp. 313–320). The Australasian Institute of Mining and Metallurgy.

Chilès, J. P., & Delfiner, P. (2012). *Geostatistics: Modeling spatial uncertainty*. Wiley.

Cowan, M. W., Beatson, R. K., Ross, H. J., Fright, W. R., McLennan, T. J., Evans, T. R., Carr, J. C., Lane, R. G., Bright, D. V., Gillman, A. J., Oshurst, P. A., & Titley, M. (2003). Practical implicit geological modelling. In S. Dominy (Ed.), *Proceedingsofthe AusIMM 5th international mining geology conference* (pp. 89–99). Australasian Institute of Mining and Metallurgy.

de la Varga, M., Schaaf, A., & Wellmann, F. (2019). GemPy 10: Open-source stochastic geological modeling and inversion. *Geoscientific Model Development, 12*(1), 1–32.

Deutsch, C. V. (2006). A sequential indicator simulation program for categorical variables with point and block data: BlockSIS. *Computers & Geosciences, 32*(10), 1669–1681.

Deutsch, C. V., & McLennan, J. A. (2007). BOUNDSIM: Implicit boundary modeling. In E. J. Magri (Ed.), *Proceedingsofthe 33rd international symposium on applications of computers and operations research in the mineral industry* (pp. 41–48). Gecamin Ltd.

Dubrule, O. (1993). Introducing more geology in stochastic reservoir modelling. In A. Soares (Ed.), *Geostatistics Tróia' 92* (pp. 351–369). Springer.

Duhart, P., Muñoz, J., Quiroz, D., Mestre, A., & Varas, G. (2018). Carta Sierra Gorda, Región de Antofagasta. Servicio Nacional de Geología y Minería, Serie Geológica Básica No. 198, 1 mapa escala 1:100.000. Santiago.

Emery, X. (2004). Properties and limitations of sequential indicator simulation. *Stochastic Environmental Research and Risk Assessment, 18*(6), 414–424.

Emery, X. (2007). Simulation of geological domains using the plurigaussian model: New developments and computer programs. *Computers and Geosciences, 33*(9), 1189–1201.

Emery, X. (2012). Cokriging random fields with means related by known linear combinations. *Computers & Geosciences, 38*(1), 136–144.

Emery, X., Arroyo, D., & Porcu, E. (2016). An improved spectral turning-bands algorithm for simulating stationary vector Gaussian random fields. *Stochastic Environmental Research and Risk Assessment, 30*(7), 1863–1873.

Emery, X., & Lantuéjoul, C. (2011). Geometric covariograms, indicator variograms and boundaries of planar closed sets. *Mathematical Geosciences, 43*(8), 905–927.

Emery, X., & Maleki, M. (2019). Geostatistics in the presence of geological boundaries: Application to mineral resources modeling. *Ore Geology Reviews, 114*, 103124.

Emery, X., & Robles, L. N. (2009). Simulation of mineral grades with hard and soft conditioning data: Application to a porphyry copper deposit. *Computational Geosciences, 13*(1), 79–89.

Emery, X., & Séguret, S. A. (2020). *Geostatistics for the mining industry—Applications to porphyry copper deposits*. CRC Press.

Gonçalves, Í. G., Kumaira, S., & Guadagnin, F. (2017). A machine learning approach to the potential-field method for implicit modeling of geological structures. *Computers & Geosciences, 103*, 173–182.

Henrion, V., Caumon, G., & Cherpeau, N. (2010). ODSIM: An object-distance simulation method for conditioning complex natural structures. *Mathematical Geosciences, 42*(8), 911–924.

Hillier, M. J., Schetselaar, E. M., de Kemp, E. A., & Perron, G. (2014). Three-dimensional modelling of geological surfaces using generalized interpolation with radial basis functions. *Mathematical Geosciences, 46*(8), 931–953.

Høyer, A. S., Vignoli, G., Hansen, T. M., Vu, L. T., Keefer, D. A., & Jørgensen, F. (2017). Multiple-point statistical simulation for hydrogeological models: 3-D training image development and conditioning strategies. *Hydrology and Earth System Sciences, 21*(12), 6069–6089.

Jessell, M. W., Ailleres, L., & de Kemp, E. A. (2010). Towards an integrated inversion of geoscientific data: What price of geology? *Tectonophysics, 490*, 294–306.

Journel, A. G., & Huijbregts, C. J. (1978). *Mining geostatistics*. Academic Press.

Journel, A. G., & Rossi, M. E. (1989). When do we need a trend model in kriging? *Mathematical Geology, 21*(7), 715–739.

Koch, J., He, X., Jensen, K. H., & Refsgaard, J. C. (2014). Challenges in conditioning a stochastic geological model of a heterogeneous glacial aquifer to a comprehensive soft data set. *Hydrology and Earth System Sciences, 18*(8), 2907–2923.

Lajaunie, C., Courrioux, G., & Manuel, L. (1997). Foliation fields and 3D cartography in geology: Principles of a method based on potential interpolation. *Mathematical Geology, 29*(4), 571–584.

Lantuéjoul, C. (2002). *Geostatistical simulation: Models and algorithms*. Springer.

Li, S. X., Knights, P., & Dunn, D. (2008). Geological uncertainty and risk: Implications for the viability of mining projects. *Journal of Coal Science and Engineering, 14*(2), 176–180.

Madani, N., & Emery, X. (2015). Simulation of geo-domains accounting for chronology and contact relationships: Application to the Río Blanco copper deposit. *Stochastic Environmental Research and Risk Assessment, 29*(8), 2173–2191.

Madani, N., & Emery, X. (2019). A comparison of search strategies to design the cokriging neighborhood for predicting coregionalized variables. *Stochastic Environmental Research and Risk Assessment, 33*(1), 183–199.

Maleki, M., Emery, X., Cáceres, A., Ribeiro, D., & Cunha, E. (2016). Quantifying the uncertainty in the spatial layout of rock type domains in an iron ore deposit. *Computational Geosciences, 20*(5), 1013–1028.

Maleki, M., Jélvez, E., Emery, X., & Morales, M. (2020). Stochastic open-pit mine production scheduling: A case study of an iron deposit. *Minerals, 10*(7), 585.

Maleki-Tehrani, M. A., Asghari, O., & Emery, X. (2013). Simulation of mineral grades and classification of mineral resources by using hard and soft conditioning data: Application to Sungun porphyry copper deposit. *Arabian Journal of Geosciences, 6*(10), 3773–3781.

Mallet, J. L. (2002). *Geomodeling*. Oxford University Press.

Manchuk, J. G., & Deutsch, C. V. (2019). Boundary modeling with moving least squares. *Computers & Geosciences, 126*, 96–106.

Mariethoz, G., & Caers, J. (2014). *Multiple-point geostatistics: Stochastic modeling with training images*. Wiley.

Matheron, G., Beucher, H., de Fouquet, C., Galli, A., Guerillot, D., & Ravenne, C. (1987). Conditional simulation of the geometry of fluvio-deltaic reservoirs. In *62nd annual technical conference and exhibition of the society of petroleum engineers. Society of Petroleum Engineers, Dallas, SPE paper 16753*.

Maxelon, M., Renard, P., Courrioux, G., Brändli, M., & Manckтelow, N. (2009). A workflow to facilitate three-dimensional geometrical modelling of complex poly-deformed geological units. *Computers & Geosciences, 35*, 644–658.

McCarthy, P. L. (2003). Managing technical risks for mine feasibility studies. In: Proceedings mining risk management conference (pp. 21–27). The Australasian Institute of Mining and Metallurgy.

Moreno, L., Sanhueza, A., Fajardo, J., Guzmán, R., Lagos, M., Nava, M., González, E., & Ruggiero, A. (2012). Mineralización Hipógena del Pórfido Paleoceno Spence. In A. H. Menzies & R. González (Eds.), *Actas del XIII Congreso Geológico Chileno* (pp. 31–33). Universidad Católica del Norte.

Ravenne, C., Galli, A., Doligez, B., Beucher, H., & Eschard, R. (2002). Quantification of facies relationships via proportion curves. In M. Armstrong, C. Bettini, N. Champigny, A. Galli, & A. Remacre (Eds.), *Geostatistics Rio 2000, Proceedings of the geostatistics sessions of the 31st international geological congress* (pp. 19–39). Springer.

Rivoirard, J. (2001). Which models for collocated cokriging? *Mathematical Geology, 33*(2), 117–131.

Rivoirard, J., Cojan, I., Renard, D., & Geffroy, F. (2008). Advances in quantification of process-based models for meandering channelized reservoirs. In J. M. Ortiz & X. Emery (Eds.), *Proceedings of the VIIIth international geostatistics congress* (pp. 607–616). Gecamin Ltd.

Royer, J. J., Mejia, P., Caumon, G., & Collon, P. (2015). 3D and 4D geomodelling applied to mineral resources exploration—An introduction. In P. Weihed (Ed.), *3D, 4D and predictive modelling of major mineral belts in Europe* (pp. 73–89). Springer.

Sánchez, L. K., Emery, X., & Séguret, S. A. (2019). 5D geostatistics for directional variables: Application in geotechnics to the simulation of the linear discontinuity frequency. *Computers and Geosciences, 133*, 104325.

Turk, G., & O'Brien, J. F. (2002). Modelling with implicit surfaces that interpolate. *ACM Transactions on Graphics, 21*(4), 855–873.

Vollgger, S. A., Cruden, A. R., Ailleres, L., & Cowan, E. J. (2015). Regional dome evolution and its control on ore-grade distribution: Insights from 3D implicit modelling of the Navachab gold deposit, Namibia. *Ore Geology Reviews, 69*, 268–284.

Wackernagel, H. (2003). *Multivariate geostatistics*. Springer.

Wellmann, J. F., Lindsay, M., Poh, J., & Jessell, M. (2014). Validating 3-D structural models with geological knowledge for improved uncertainty evaluations. *Energy Procedia, 59*, 374–381.

Wellmann, F., & Caumon, G. (2018). 3-D Structural geological models: Concepts, methods, and uncertainties. *Advances in Geophysics, 59*, 1–121.

CAPÍTULO TERCERO

3. CONCLUSIONES Y TRABAJO FUTURO

3.1. CONCLUSIONES GENERALES

Se ha propuesto una adaptación de la simulación implícita de contactos para tener en cuenta dos fuentes de información al simular unidades geológicas en yacimientos mineros: información dura que se origina a partir de datos de perforaciones e información blanda de un modelo geológico interpretativo del yacimiento. Estos últimos se introducen como una covariable que se correlaciona de forma cruzada con la variable principal asociada con la información dura. Al reducir la meseta del variograma cruzado entre ambas variables, se puede controlar el nivel de confianza de la información blanda: un coeficiente de reducción de escala igual a 1 produce la semejanza máxima entre el modelo interpretativo y las unidades geológicas simuladas, mientras que un coeficiente igual a 0 hace que el modelo interpretativo no influye en la simulación. La elección de dicho coeficiente puede basarse en consideraciones geológicas y / o técnicas de validación cruzada.

El algoritmo propuesto se ha aplicado en dos casos de estudio, uno sintético y otro correspondiente a un depósito de pórfido de cobre. En ambos casos, las unidades simuladas reproducen la zonificación espacial del modelo geológico interpretativo. La implementación también ha revelado dificultades relacionadas con el cálculo de la distancia en el fondo del sondaje hasta el límite de la unidad, la transformación de valores normales, el análisis variográfico y la coherencia entre la información dura y blanda.

3.2. RECOMENDACIONES Y TRABAJO FUTURO

Como perspectivas para trabajos futuros, uno puede imaginar que el coeficiente utilizado para cuantificar la confianza en el modelo geológico interpretativo puede variar en el espacio, o que los datos deben ser regionalizados en un espacio de cinco dimensiones para dar cuenta no solo de sus posiciones geográficas (coordenadas este, norte y elevación), sino también para la dirección (azimut e inclinación) a lo largo de la cual se calculan las distancias a los límites de la unidad.

4. BIBLIOGRAFÍA

Alabert, F. (1987). Stochastic imaging of spatial distributions using hard and soft information. MSc. dissertation, Stanford University.

Amarante, F. A. N., Rolo, R. M., Coimbra Leite Costa, J. F. (2021). Boundary simulation-a hierarchical approach for multiple categories. Applied Earth Science: Transactions of the Institute of Mining and Metallurgy, 130(2), 114-130.

Armstrong, M., Galli, A., Beucher, H., Loc'h, G., Renard, D., Doligez, B., Eschard, R., Geffroy, F. (2011). Plurigaussian Simulations in Geosciences. Springer, Berlin.

Aug, C., Chilès, J. P., Courrioux, G., Lajaunie, C. (2005). 3D geological modelling and uncertainty: The potential-field method. In: Leuangthong, O., Deutsch, C. V. (eds.) Geostatistics Banff 2004. Springer, Dordrecht, pp. 145-154.

Benito Garcia-Morales, M., Beucher, H., Geffroy, F., Doligez, B. (2003). Object-based simulations in fluvial environment at the reservoir scale and at a local scale. In: Proceedings of the AAPG annual convention. Salt Lake City, Utah. AAPG Search and Discovery Article #90013, 7 p.

Berry, M., McCarthy, P. (2006). Practical consequences of geological uncertainty. In: Proceedings of the Sixth International Mining Geology Conference. The Australasian Institute of Mining and Metallurgy, Melbourne, pp. 253-258.

Beucher, H., Galli, A., Le Loc'h, G., Ravenne, C. (1993). Including a regional trend in reservoir modelling using the truncated Gaussian method. In: Soares, A. (ed.) Geostatistics Tróia' 92. Springer, Dordrecht, pp. 555-566.

Beucher, H., García-Morales, M., Geffroy, F. (2005) Fitting the Boolean parameters in a non-stationary case. In: Leuangthong, O., Deutsch, C.V. (eds.) Geostatistics Banff 2004. Springer, Dordrecht, pp. 569-578.

Boric, R., Díaz, F., Maksaev, V. (1990). Geología y yacimientos metalíferos de la Región de Antofagasta. Servicio Nacional de Geología y Minería, Boletín No. 40, 246 p.

Bunker, E., Blundy, J., Cooper, F., Condon, D., Tapster, S. (2017). Textural, spatial and temporal variation within the igneous suites of the Spence porphyry copper deposit, northern Chile. Applied Earth Science, 126(2), 47-48.

Cáceres, A., Emery, X., Aedo, L., Gálvez, O. (2011). Stochastic geological modeling using implicit boundary simulation. In: Beniscelli, J., Kuyvenhoven, R., Hoal, K. O. (eds.) Proceedings of the 2nd International Seminar on Geology for the Mining Industry. Gecamin Ltda, Santiago, 10 p.

Calcagno, P., Chilès, J. P., Courrioux, G., Guillen, A. (2008). Geological modelling from field data and geological knowledge. Part I. Modelling method coupling 3D potential-field interpolation and geological rules. Physics of the Earth and Planetary Interiors, 171, 147-157.

Carle, S. F., Fogg, G. E. (1997). Modeling spatial variability with one and multidimensional continuous-lag Markov chains. Mathematical Geology, 29(7), 891-918.

Carle, S. F., Fogg, G. E. (2020). Integration of soft data into geostatistical simulation of categorical variables. Frontiers in Earth Science, 8, 449.

Carr, J. C., Beatson, R. K., Cherrie, J. B., Mitchell, T. J., Fright, W. R., McCallum, B. C., Evans, T. R. (2001). Reconstruction and representation of 3D objects with radial basis functions. In: Pocock, L. (ed.) Proceedings of the 28th Annual Conference on Computer Graphics and Interactive Techniques. Association for Computing Machinery, New York, pp. 67-76.

Caumon, G., Gray, G., Antoine, C., Titeux, M. O. (2013). Three-dimensional implicit stratigraphic model building from remote sensing data on tetrahedral meshes: Theory and application to a regional model of La Popa Basin, NE Mexico. IEEE Transactions on Geoscience and Remote Sensing, 51(3), 1613-1621.

Chilès, J. P., Aug, C., Guillen, A., Lees, T. (2004). Modelling the geometry of geological units and its uncertainty in 3D from structural data: The potential-field method. In: Dimitrakopoulos, R., Ramazan, S. (eds.), Orebody Modelling and Strategic Mine Planning. The Australasian Institute of Mining and Metallurgy, Carlton, Victoria, pp. 313-320.

Chilès, J. P., Delfiner, P. (2012). Geostatistics: Modeling Spatial Uncertainty. Wiley, New York.

Cowan, M. W., Beatson, R. K., Ross, H. J., Fright, W. R., McLennan, T. J., Evans, T. R., Carr, J. C., Lane, R. G., Bright, D. V., Gillman, A. J., Oshurst, P.A., Titley, M. (2003). Practical implicit geological modelling. In: Dominy, S. (ed.) Proceedings of the AusIMM 5th International Mining Geology Conference. Australasian Institute of Mining and Metallurgy, Carlton, pp. 89-99.

De la Varga, M., Schaaf, A., Wellmann, F. (2019). GemPy 1.0: Open-source stochastic geological modeling and inversion. Geoscientific Model Development, 12(1), 1-32.

Deutsch, C. V. (2006) A sequential indicator simulation program for categorical variables with point and block data: BlockSIS. Computers & Geosciences, 32(10), 1669-1681.

Deutsch, C. V., McLennan, J. A. (2007). BOUNDSIM: Implicit boundary modeling. In: Magri, E. J. (ed.) Proceedings of the 33rd International Symposium on Applications of Computers and Operations Research in the Mineral Industry. Gecamin Ltda, Santiago, pp. 41-48.

Dubrule, O. (1993). Introducing more geology in stochastic reservoir modelling. In: Soares, A. (ed.) Geostatistics Tróia' 92. Springer, Dordrecht, pp. 351-369.

Duhart, P., Muñoz, J., Quiroz, D., Mestre, A., Varas, G. (2018). Carta Sierra Gorda, Región de Antofagasta. Servicio Nacional de Geología y Minería, Serie Geológica Básica No. 198, 1 mapa escala 1:100.000. Santiago.

Emery, X. (2004). Properties and limitations of sequential indicator simulation. Stochastic Environmental Research and Risk Assessment, 18(6), 414-424.

Emery, X. (2007). Simulation of geological domains using the plurigaussian model: New developments and computer programs. Computers and Geosciences, 33(9), 1189-1201.

Emery, X. (2012). Cokriging random fields with means related by known linear combinations. Computers & Geosciences, 38(1), 136-144.

Emery, X., Arroyo, D., Porcu, E. (2016). An improved spectral turning-bands algorithm for simulating stationary vector Gaussian random fields. Stochastic Environmental Research and Risk Assessment, 30(7), 1863-1873.

Emery, X., Lantuéjoul, C. (2011). Geometric covariograms, indicator variograms and boundaries of planar closed sets. Mathematical Geosciences, 43(8), 905-927.

Emery, X., Maleki, M. (2019). Geostatistics in the presence of geological boundaries: Application to mineral resources modeling. Ore Geology Reviews, 114, article 103124.

Emery, X., Robles, L. N. (2009). Simulation of mineral grades with hard and soft conditioning data: Application to a porphyry copper deposit. Computational Geosciences, 13(1), 79-89.

Emery, X., Séguret, S.A. (2020). Geostatistics for the Mining Industry - Applications to Porphyry Copper Deposits. CRC Press, Boca Raton.

Galli, A., Beucher, H., Le Loc'h, G., Doligez, B. (1994). The pros and cons of the truncated gaussian method. In: Armstrong et al. (eds) Geostatistical simulations. Kluwer, Dordrecht, 217-233p.

Gonçalves, Í. G., Kumaira, S., Guadagnin, F. (2017). A machine learning approach to the potential-field method for implicit modeling of geological structures. Computers & Geosciences, 103, 173-182.

Henrion, V., Caumon, G., Cherpeau, N. (2010). ODSIM: An object-distance simulation method for conditioning complex natural structures. Mathematical Geosciences, 42(8), 911-924.

Hillier, M. J., Schetselaar, E. M., de Kemp, E. A., Perron, G. (2014). Three-dimensional modelling of geological surfaces using generalized interpolation with radial basis functions. Mathematical Geosciences, 46(8), 931-953.

Høyer, A. S., Vignoli, G., Hansen, T. M., Vu, L. T., Keefer, D. A., Jørgensen, F. (2017). Multiple-point statistical simulation for hydrogeological models: 3-D training image development and conditioning strategies. Hydrology and Earth System Sciences, 21(12), 6069-6089.

Jessell, M. W., Ailleres, L., de Kemp, E. A. (2010). Towards an integrated inversion of geoscientific data: what price of geology? Tectonophysics, 490, 294-306.

Journel, A. G., Huijbregts, C. J. (1978). Mining Geostatistics. Academic Press, London.

Journel, A. G., Rossi, M. E. (1989). When do we need a trend model in kriging? Mathematical Geology, 21(7), 715-739.

Koch, J., He, X., Jensen, K. H., Refsgaard, J. C. (2014). Challenges in conditioning a stochastic geological model of a heterogeneous glacial aquifer to a comprehensive soft data set. Hydrology and Earth System Sciences, 18(8), 2907-2923.

Lajaunie, C., Courrioux, G., Manuel, L. (1997). Foliation fields and 3D cartography in geology: Principles of a method based on potential interpolation. Mathematical Geology, 29(4), 571-584.

Lantuéjoul, C. (2002). Geostatistical Simulation: Models and Algorithms. Springer, Berlin.

Li, S. X., Knights, P., Dunn, D. (2008). Geological uncertainty and risk: implications for the viability of mining projects. Journal of Coal Science and Engineering, 14(2), 176-180.

Madani, N., Emery, X. (2015). Simulation of geo-domains accounting for chronology and contact relationships: application to the Río Blanco copper deposit. Stochastic Environmental Research and Risk Assessment, 29(8), 2173-2191.

Madani, N., Emery, X. (2019). A comparison of search strategies to design the cokriging neighborhood for predicting coregionalized variables. Stochastic Environmental Research and Risk Assessment, 33(1), 183-199.

Maleki, M., Emery, X., Cáceres, A., Ribeiro, D., Cunha, E. (2016). Quantifying the uncertainty in the spatial layout of rock type domains in an iron ore deposit. Computational Geosciences, 20(5), 1013-1028.

Maleki, M., Jélvez, E., Emery, X., Morales, M. (2020). Stochastic open-pit mine production scheduling: a case study of an iron deposit. Minerals, 10(7), article 585.

Maleki-Tehrani, M. A., Asghari, O., Emery, X. (2013). Simulation of mineral grades and classification of mineral resources by using hard and soft conditioning data: Application to Sungun porphyry copper deposit. Arabian Journal of Geosciences, 6(10), 3773-3781.

Mallet, J. L. (2002). Geomodeling. Oxford University Press, New York.

Manchuk, J. G., Deutsch, C. V. (2019). Boundary modeling with moving least squares. Computers & Geosciences, 126, 96-106.

Mariethoz, G., Caers, J. (2014). Multiple-Point Geostatistics: Stochastic Modeling with Training Images. Wiley, New York.

Matheron, G., Beucher, H., de Fouquet, C., Galli, A., Guerillot, D., Ravenne, C. (1987). Conditional simulation of the geometry of fluvio-deltaic reservoirs. In: 62nd Annual Technical Conference and Exhibition of the Society of Petroleum Engineers. Society of Petroleum Engineers, Dallas, SPE paper 16753.

Maxelon, M., Renard, P., Courrioux, G., Brändli, M., Mancktelow, N. (2009). A workflow to facilitate three-dimensional geometrical modelling of complex poly-deformed geological units. Computers & Geosciences, 35, 644-658.

McCarthy, P. L. (2003). Managing technical risks for mine feasibility studies. In: Proceedings Mining Risk Management Conference, The Australasian Institute of Mining and Metallurgy, Melbourne, pp. 21-27.

McLennan, J., Deutsch, C., (2006). Implicit boundary modeling (boundsim). Centre for Computational Geostatistics, 2006.

Moreno, L., Sanhueza, A., Fajardo, J., Guzmán, R., Lagos, M., Nava, M., González, E., Ruggiero, A. (2012). Mineralización Hipógena del Pórfido Paleoceno Spence. In: Menzies, A. H., González, R. (eds.) Actas del XIII Congreso Geológico Chileno. Universidad Católica del Norte, Antofagasta, pp. 31-33.

Pyrcz, M., Deutsch, C. (2014). Geostatistical Reservoir Modeling. 2th edition. Oxford University Press. 448p.

Ravenne, C., Galli, A., Doligez, B., Beucher, H., Eschard, R. (2002). Quantification of facies relationships via proportion curves. In: Armstrong, M., Bettini, C., Champigny, N., Galli, A., Remacre, A. (eds.) Geostatistics Rio 2000, Proceedings of the Geostatistics Sessions of the 31st International Geological Congress. Springer, New York, pp. 19-39.

Remy, N., Boucher, A., Wu, J. (2009). Applied geostatistics with SGeMS: a user's guide. Cambridge University Press.

Rivoirard, J. (2001). Which models for collocated cokriging? Mathematical Geology, 33(2), 117-131.

Rivoirard, J., Cojan, I., Renard, D., Geffroy, F. (2008). Advances in quantification of process-based models for meandering channelized reservoirs. In: Ortiz, J. M., Emery, X. (eds.) Proceedings of the VIIIth International Geostatistics Congress. Gecamin Ltda, Santiago, pp. 607-616.

Royer, J. J., Mejia, P., Caumon, G., Collon, P. (2015) 3D and 4D geomodelling applied to mineral resources exploration - An introduction. In: Weihed, P. (ed.) 3D, 4D and Predictive Modelling of Major Mineral Belts in Europe. Springer, Cham, pp. 73-89.

Sánchez, L. K., Emery, X., Séguret, S. A. (2019). 5D geostatistics for directional variables: Application in geotechnics to the simulation of the linear discontinuity frequency. Computers and Geosciences, 133, article 104325.

Strebelle, S. (2002). Conditional simulation of complex geological structures using multiple-point statistics. Mathematical Geology. Vol. 34(1), 1-21p.

Turk, G., O'Brien, J. F. (2002) Modelling with implicit surfaces that interpolate. ACM Transactions on Graphics, 21(4), 855-873.

Vollgger, S. A., Cruden, A. R., Ailleres, L., Cowan, E. J. (2015). Regional dome evolution and its control on ore-grade distribution: Insights from 3D implicit modelling of the Navachab gold deposit. Namibia. Ore Geology Reviews, 69, 268-284.

Wackernagel, H. (2003). Multivariate Geostatistics. Springer Berlin.

Wellmann, J. F., Lindsay, M., Poh, J., Jessell, M. (2014). Validating 3-D structural models with geological knowledge for improved uncertainty evaluations. Energy Procedia, 59, 374-381.

Wellmann, F., Caumon, G. (2018). 3-D Structural geological models: Concepts, methods, and uncertainties. Advances in Geophysics, 59, 1-121